MOISTURE MOVEMENT FROM A SUBSURFACE IRRIGATION SOURCE

Dissertation for the Degree of Ph. D.

MICHIGAN STATE UNIVERSITY
THEODORE L. LOUDON

1973

This is to certify that the

thesis entitled

MOISTURE MOVEMENT

FROM A SUBSURFACE IRRIGATION SOURCE

presented by

Theodore L. Loudon

has been accepted towards fulfillment
of the requirements for

Ph.D. degree in
Agricultural Engineering

E. R. Kadden

Major professor

Date Nov. 7, 1973

O-7639

ABSTRACT

MOISTURE MOVEMENT
FROM A SUBSURFACE IRRIGATION SOURCE

By

Theodore L. Loudon

Moisture movement from a subsurface irrigation source was simulated in a large soil chamber with water entering soil at an initially uniform moisture content. The differential equation describing one-dimensional radial flow was solved numerically using a predictor-corrector method for conditions along each of the three major directions from the source (horizontal, vertically up, and vertically down). Calculated results were compared with experimental results.

For the silty sand used in this study, the one-dimensional model reasonably predicted the horizontal advance of the wetting front, provided that the growth of the saturated zone around the source was known for use in the model. Horizontal advance was related to time by an equation of the form $r = at^n$, and the value of n was found to be about 0.47. Vertical advance at large times was not of this form.

The one-dimensional equation does not appear to be valid for predicting vertical advance either up or down from the source. A two-dimensional solution for the entire flow region is necessary. However,

if depth of placement of subsurface irrigation laterals is determined by considerations other than the movement of the wetting front during infiltration, it may be possible to determine proper lateral spacing using a one-dimensional solution of the flow equation.

Approved E N Kidder 11/3/73
Major Professor

Approved B A Stout
Department Chairman

MOISTURE MOVEMENT
FROM A SUBSURFACE IRRIGATION SOURCE

By

Theodore L. Loudon

A DISSERTATION

Submitted to

Michigan State University

in partial fulfillment of the requirements

for the degree of

DOCTOR OF PHILOSOPHY

Department of Agricultural Engineering

1973

ACKNOWLEDGEMENTS

The author wishes to acknowledge the financial support received from the Agricultural Engineering Department during his graduate study and to thank Dr. B. A. Stout, Chairman, for his patience and faith that the project would be completed. Thanks are extended to the author's graduate committee -- Professor E. H. Kidder, Chairman, Dr. M. E. Merva, Dr. John L. Gill, and Dr. R. J. Kunze -- for their assistance, but especially to Dr. Kunze for his extensive help in supplying equipment and personal guidance which made the project possible. Fellow graduate student Levern Faidley is thanked for many hours of assistance, particularly during the experimental aspects of the study. Most of all, a special thank you goes to the author's wife, Barb, for her bountiful understanding and encouragement throughout the project and for her assistance in typing the manuscript.

TABLE OF CONTENTS

LIST OF TABLES

LIST OF FIGURES

LIST OF SYMBOLS

A	polynomial coefficient
B	polynomial coefficient
C	polynomial coefficient
C	water capacity of soil
D	soil moisture diffusivity
H	total hydraulic head
I	radiation intensity
I_o	radiation intensity emitted from source
K	unsaturated hydraulic conductivity
N	scaler counts of radiation
R	polynomial term
S	percent saturation
T_t	radiation counting time
a	coefficient in parabolic equation
a_0	polynomial coefficient
a_1	polynomial coefficient
h	capillary pressure head
h_i	capillary pressure head, initial
i	subscript referring to position, r direction
j	subscript referring to time
n	exponent of time in parabolic equation
r	radial distance
r_o	radius of source or saturated region
s	thickness of material in radiation path
t	time

t_d dead time or radiation counting equipment

x horizontal cartesian coordinate, positive right

z vertical cartesian coordinate, positive down

η porosity of soil

θ volumetric moisture content

θ_i initial moisture content

θ_s moisture content at saturation

θ_t moisture content at time t

θ_x moisture content at a particular position, x

λ variable for Boltzmann transformation

μ mass absorption coefficient

μ_s mass absorption coefficient for soil

μ_w mass absorption coefficient for water

ν soil moisture flux

ρ density

σ standard deviation

φ angular coordinate in polar coordinate system, $\varphi = 0$ along positive z axis

I. INTRODUCTION

As the world population continues to increase, the demand for agricultural products increases as well. To meet the increased demand, the use of irrigation to provide a better plant growth environment and higher crop yields is necessary where natural precipitation may not always provide adequate moisture. Increased use of water is expected for supplemental irrigation in humid regions and to bring new land into production in arid areas. The same forces of population and increasing consumption which drive agricultural product demand upward cause other water users to increase their demands, too. Since irrigation is a high consumptive use of water, competition for our limited water resources makes it imperative that engineers search for more efficient methods of irrigation.

The luxury of having machines do work which was once done by human labor has multiplied man's leisure hours and increased the use of recreational facilities. Certain of these facilities require lush grass--irrigated and fertilized to maintain its vigor. For heavily used recreational areas, an irrigation system which will not interrupt use of the facility or be damaged by traffic is advantageous.

Another factor necessitating the development of improved irrigation systems is the cost and scarcity of labor. Today's high wages make it

necessary to select systems which allow easy automation.

Subsurface irrigation, the delivery of water directly to the root zone of the plant without wetting the soil surface, shows promise as an efficient and labor-saving method. It has been practiced for many years in isolated geologic conditions where a relatively impermeable layer within a few feet of the soil surface reduced percolation and formed a saturated region from which water moved into the root zone by capillarity. Seepage from parallel ditches supplied water to maintain the high water table.

The development of a variety of plastic pipes has added a new dimension to subsurface irrigation. Water can be supplied directly to the root zone from a system of closely spaced perforated or porous-wall pipe placed at shallow depths. Water passes through a buried main line to buried plastic laterals having either closely spaced orifices or porous sidewalls which emit water continuously along the length of the lateral. Orifice inserts of various geometries have been used to help regulate flow and reduce plugging of perforated pipe. Small amounts of water flow directly into the root zone, and with the exception of a region immediately around the lateral, water moves in the soil in an unsaturated state as a result of capillary forces. Aeration within the root zone is maintained.

Advantages cited for these new subsurface irrigation systems are rather dramatic. They include: application of water directly to the

root zone, decreased evaporation loss, increased irrigation efficiency, decreased tillage, continuation of cultural practices while irrigation is in progress, direct soil application of chemicals with irrigation water, and equal or increased yields.

In the past few years, researchers have been working to evaluate the performance of plastic pipe subirrigation systems. Much of this work has been summarized by Hanson et al. (1970), Braud (1970), Whitney (1970), Edwards et al. (1970), and Davis and Nelson (1970). Early work on the hydraulics of perforated plastic pipe systems was done by Zetzsche (1964) and Bryan and Baker (1964). Hydraulic characteristics of orifice and pipe systems have also been reported by Hoskyn and Bryan (1969), Zetzsche and Newman (1968), Lo (1968), and Wilke (1970).

Field studies comparing subsurface irrigated crop yields with other irrigation methods have been reported by Braud, Hernandez and Brown (1969), Hanson and Williams (1968), and Busch and Kneebone (1966). More recently, Patterson (1972), Vaziri (1972), and Hiler and Howell (1972) have also reported results of field tests to evaluate the crop yield response to subsurface irrigation. In general, yields are comparable to those resulting from other irrigation methods except that Patterson found trickle irrigation produced superior yields of sweet corn and onions on the basis of pounds of yield per acre-inch of water.

Several investigators have conducted laboratory studies to evaluate the water movement into a soil from a point or cylindrical source

simulating a subsurface irrigation system. Busch and Kneebone (1966) conducted laboratory tests using pressures of 15 to 25 in. of water in perforated pipe and reported the results on wetting front advance in three directions--horizontally, vertically up, and vertically down--for two soils in the form

$$r = at^n \qquad (1)$$

where r is the radial distance from the source to the edge of the wetting front, t is the time from the beginning of irrigation, and a and n are constants, depending upon the direction of movement considered, soil characteristics, orifice size, and pressure.

Smith (1966) and Whitney et al. (1966) also expressed visible wetting front advance data in the form of equation 1. Since the parameters a and n vary with the extent of positive water pressure in the soil outside the source, the soil characteristics, and the direction of movement, results of this nature are difficult to extrapolate. The zone of positive pressure in the soil can be large if orifices are used with pipe pressures of more than a few inches of water.

In a laboratory study to determine proper depth and spacing of subsurface irrigation laterals, Edwards and Goel (1971) placed perforated pipes 12 and 18 inches below soybean plants in a soil bin. They used electrical resistance blocks to evaluate soil moisture extraction patterns from the greenhouse bins irrigated by a subsurface source. For the silty clay loam soil used, they recommended the 18-inch lateral

depth over the 12 and suggested spacing equal to twice the depth.

Researchers working on subsurface irrigation have been generally enthusiastic about the potential of the method. Orifice plugging has been a problem, but fine filtration of the water and the use of orifice inserts or porous-wall pipe may solve this problem. Recommendations for lateral depth and spacing have been made for particular situations, but further work is needed to develop a general procedure for determining lateral placement.

II. DEVELOPMENT OF OBJECTIVES

Design Procedures for Subsurface Irrigation

There are two phases to the design of subsurface irrigation systems. One involves the design of the water distribution system used to bring the water to any given orifice or point along porous pipe from which it moves into the soil. The design of supply laterals is basically a problem of unsteady pipe flow. Zetzsche and Newman (1968) considered the design of laterals with uniformly spaced orifices along plastic pipe.

Wilke (1970) conducted studies to determine the hydraulic roughness and general performance of Micro-Por^{tm} porous-wall pipe. He found that this material has a slightly greater hydraulic roughness than smooth-wall pipe. Relatively uniform discharge rates along laterals are possible, but Wilke suggested that the permeability of the pipe wall should be reduced. These two studies, along with engineering techniques for pipe flow design, provide the basic information required for approaching the pipe flow aspect of subsurface irrigation system design.

The second phase of subsurface irrigation design involves the infiltration pattern as water moves from the lateral into the soil. The proper depth and spacing for subsurface irrigation laterals depend on

the size and shape of the soil region around each source or lateral which is wetted during irrigation. This wetted pattern depends on the length of time the water is infiltrating, the flow rate from the lateral, the antecedent moisture conditions in the soil, and the unsaturated conductivity (or diffusivity) function for the particular soil. Moisture movement from a buried source has generally been considered unsaturated flow; but if the flux from the source is greater than can flow under unsaturated conditions in soil, a saturated zone develops around the source.

To determine the wetted pattern for new installations, it has been common to install a section of lateral, run it for a period of time, and excavate a cross-section to look at the wetted region (Trambley, undated). Many surface irrigation systems have also required field infiltration trials associated with their design in the past. The basic theory for unsaturated water movement in soils is fairly well developed, and progress is being made toward the determination of soil moisture flow coefficients. Therefore, it is desirable to carry out investigations to apply available theory to problems such as subsurface irrigation and develop models describing the flow. Models for prediction of soil moisture movement will allow engineers to evaluate various operation and design variations prior to field installation.

Predicting Soil Moisture Movement--State of the Art

Both analytical and numerical solutions have been published for unsaturated flow problems in soils. The analytical solutions require rather involved mathematical techniques but provide a better understanding of the flow system than numerical solutions, at least for the specific conditions for which solutions can be found. Analytical approaches require the expression of soil moisture parameters in equation form as a function of soil moisture content. The solution is then valid only for soils with parameters which fit the chosen function.

The numerical approach to moisture flow problems requires expressing the differential equations derived in Chapter III in some tractable finite difference form. While numerical solutions are less informative as far as understanding the flow system is concerned, they are more easily adapted to individual soil conditions. Soil parameters can be expressed as discrete values determined from field or laboratory experiments and need not fit a specific mathematical function when used with numerical techniques.

Most of the present knowledge for solution of soil moisture flow equations is the result of analysis of one-dimensional flow such as water movement into a vertical soil column with shallow water ponded on the surface. Analytical solutions to one-dimensional infiltration have been developed by Philip (1969a) and Parlange (1971). Numerous numerical solutions for one-dimensional flow have been summarized by

Freeze (1969). The most widely used approach seems to be that given by Hanks and Bowers (1962).

Analytical solutions to two-dimensional problems such as infiltration from a furrow have been published by Raats (1970) and Parlange (1972). Philip (1969b) gave analytical solutions to certain situations of infiltration from buried point and line sources. His solutions were only for time near zero and for large times approaching infinity. Parlange (1972) and Raats (1972) also derived analytical solutions for infiltration from buried point sources. Using techniques suggested by Raats (1970), Gilley and Allred (1972) developed an analytical solution to steady state flow from a subsurface line source and compared the results of their solution with recommendations for depth and spacing of subsurface irrigation laterals which have resulted from various field and laboratory trials.

Most of the published solutions to two-dimensional problems using numerical techniques involve the use of the alternating direction implicit procedure. Two works of this nature are Rubin (1968) and Brutsaert (1971). While solutions to flow problems are not lacking in the literature, few numerical or analytical solutions have been compared with direct laboratory or field measurements.

Determination of the unsaturated hydraulic conductivity or diffusivity for a particular soil must precede the application of available methods for solving the differential equation describing soil moisture

movement. Soil physicists have developed a number of methods for measuring these parameters both in the field and in the laboratory. Klute (1972) has summarized the rather large number of published papers dealing with determination of these parameters and has suggested the most useful methods for certain field and laboratory situations. The various methods he discussed are divided into three categories: steady state methods, unsteady state methods, and methods involving calculation from water retention data. Klute makes an interesting observation regarding the accuracy required in the conductivity function for use in predicting field soil moisture movement: "In view of the variability of soils in the field, a high order of accuracy in the conductivity function is not essential for meaningful application of computed results to field problems."

Methods used in this study are described in detail in Chapter V.

Objectives

The flow from a subsurface irrigation lateral is considered here as a problem of two-dimensional infiltration from a cylindrical source. These laterals may be operated continuously, resulting in nearly steady state conditions, but are more likely to be operated intermittently. Therefore, a design procedure based on analysis of the unsteady flow situation is needed. Once developed, this should make it convenient to analyze flow under a variety of soil conditions and system operation schemes.

After analyzing the numerical solutions available for potential use in solving equations of the type describing soil moisture movement and the progress which is being made in characterizing the coefficients governing soil moisture flow, the author developed the following objectives for a study which could have application to design procedures for subsurface irrigation:

1. To develop numerical solutions for the differential equation describing flow from a buried cylindrical source.

2. To conduct laboratory experiments on infiltration into soil at a uniform initial moisture content from a buried porous pipe.

3. To compare the results of calculated and experimental infiltration.

III. THEORY AND MATHEMATICAL MODELS

Development of Equations

Moisture movement in the root zone of agricultural soils is generally a case of unsteady flow in partially saturated porous media. It occurs as a result of moisture application--either by natural precipitation or by irrigation--or as a result of drainage of excess water to natural or artificial drainage-ways present in the soil. Both processes may occur simultaneously, but this results in a situation which is much more difficult to analyze, so it is often assumed that only drainage or only imbibition is occurring.

Unsaturated flow is actually a multi-phase flow situation because as water enters the soil, it replaces air which must flow from the region where it is replaced. Generally, the liquid phase is of primary interest, and the effects of the gaseous phase are assumed to be negligible. However, air which cannot escape as it is displaced by the advancement of infiltrating water would have to be taken into account in analyzing the flow process. Recently, Vachaud et al. (1973) measured soil air pressures in a vertical laboratory sand column and found them to differ from atmospheric pressure external to the column. For the present study, the air phase was neglected.

The basis for describing soil moisture flow mathematically is the Darcy equation

$$\nu = - K \nabla H \tag{2}$$

where ν is the moisture flux, K is the hydraulic conductivity, and H is the total hydraulic head driving flow. While the Darcy equation was originally developed for saturated flow, it is customary to use it for unsaturated flow by substituting the moisture content dependent unsaturated hydraulic conductivity for the saturated conductivity. Although flow which exhibits non-Darcy behavior is believed to exist in soils, Kirkham and Powers (1972) say that the extent to which it is encountered is not fully understood and that at least for many flow problems, Darcy's law leads to valid results.

In using the Darcy equation for unsaturated flow, the hydraulic head is given by

$$H = h + z \tag{3}$$

where h is the capillary pressure head and z is the gravitational component of the head. Applying the principle of continuity to soil moisture flow gives

$$\frac{\partial \theta}{\partial t} = - \nabla \cdot \nu \tag{4}$$

where θ is the volumetric soil moisture content and t is time. Equation 4 can be combined with the Darcy equation to give the basic equation for soil moisture flow

$$\frac{\partial \theta}{\partial t} = \nabla \cdot (K \nabla H) = \nabla \cdot (K \nabla h) + \frac{\partial K}{\partial z} \qquad (5)$$

where K is the unsaturated hydraulic conductivity and the term $\frac{\partial K}{\partial z}$ results from the use of h + z for H and represents the gravitational influence on the flow.

The hydraulic conductivity of soils generally depends on the direction of flow, and to be exact K would have to be expressed as a second-order tensor. Methods for determining the off-diagonal components of the conductivity tensor are just being researched (Cisler, 1972). In analyzing soil moisture flow, most authors consider the off-diagonal elements of the conductivity tensor to be zero and further assume isotropic soil, equating the major diagonal elements of the tensor. This simplification has been made for the purpose of this study, and the unsaturated conductivity has been considered as a scaler point function, dependent on θ only.

Equation 5 can be converted into a form which Philip (1969a) indicated is more tractable by introducing the soil moisture diffusivity, D, defined by

$$D = K \frac{dh}{d\theta} = \frac{K}{C} \qquad (6)$$

where C is known as the water capacity of the soil. Equation 5 then becomes

$$\frac{\partial \theta}{\partial t} = \nabla \cdot (D \nabla \theta) + \frac{\partial K}{\partial z} \quad . \qquad (7)$$

Both C and D, like K, vary with moisture content.

The range of application of equations 5 and 7 is not the same. Equation 5 is the more general, and in addition to applying to homogeneous soil, it is also applicable to nonhomogeneous soils if the nonhomogeneities can be divided into zones and a separate K function used for each zone. Equation 5 can also be applied when h becomes positive, i.e. where the soil is saturated by using the saturated hydraulic conductivity for K and the positive pressure gradient. However, equation 7, where the gradient is expressed as a concentration gradient, can be used only for homogeneous soils and unsaturated conditions. Equation 7 is of the diffusion or heat conduction form but has two complications which add greatly to the difficulty of its solution. One is a first-order term representing the influence of gravity on the infiltration process. Secondly, the equation is nonlinear because D and K are highly dependent on θ.

Another complication associated with the use of either of the equations is that both the $D(\theta)$ and $K(\theta)$ relations exhibit hysteresis. The parameters can be assumed single-valued functions of θ for soils which are only wetting or only drying. Equations 5 and 7 are not easily applied in situations such as redistribution where wetting and draining occur simultaneously because of the hysteresis in D and K. Further, in applying equations 5 and 7, it must be assumed that the flow is isothermal, that no swelling or shrinking of the soil mass occurs, and that chemical and biological effects are negligible.

Philip (1969a) has pointed out that the initial stage of flow from a buried line source involves nearly radially symmetric flow since the gravitational influence on the early flow is small. For ease in describing boundary conditions, it is logical to use equation 7 in polar coordinate form to describe moisture movement from a buried pipe, thus

$$\frac{\partial\theta}{\partial t} = \frac{1}{r}\frac{\partial}{\partial r}\left(D\, r \frac{\partial\theta}{\partial r}\right) + \frac{1}{r^2}\frac{\partial}{\partial\varphi}\left(D \frac{\partial\theta}{\partial\varphi}\right) - \frac{\partial K}{\partial z} \qquad (8)$$

where r is the radial space coordinate, φ is the angular space coordinate, and z is positive downward causing the sign change from equation 7. Using the chain rule

$$\frac{\partial K}{\partial z} = \frac{\partial K}{\partial r} \cdot \frac{\partial r}{\partial z} + \frac{\partial K}{\partial\varphi} \cdot \frac{\partial\varphi}{\partial z} \quad . \qquad (9)$$

Expressing r as $(x^2 + z^2)^{\frac{1}{2}}$, letting $\varphi = 0$ along the positive z axis, and increasing φ counter-clockwise, one finds

$$\frac{\partial r}{\partial z} = \cos\varphi \qquad (10)$$

and

$$\frac{\partial\varphi}{\partial z} = -\frac{1}{r}\sin\varphi \quad . \qquad (11)$$

Using equations 9, 10, and 11 in equation 8 results in

$$\frac{\partial\theta}{\partial t} = \frac{1}{r}\frac{\partial}{\partial r}\left(D\, r \frac{\partial\theta}{\partial r}\right) + \frac{1}{r^2}\frac{\partial}{\partial\varphi}\left(D \frac{\partial\theta}{\partial\varphi}\right) - \cos\varphi \frac{\partial K}{\partial r} + \frac{1}{r}\sin\varphi \frac{\partial K}{\partial\varphi} \qquad (12)$$

as the equation for two-dimensional flow in polar coordinates. For zero pressure, i.e. a saturated concentration condition just outside

the source and infiltration into a soil of uniform initial moisture content, the initial and boundary conditions can be expressed as

$$\begin{aligned} \theta &= \theta_i, \quad r > 0, \quad t = 0 \\ \theta &= \theta_s, \quad r = r_o, \quad t > 0 \\ \theta &= \theta_i, \quad r \to \infty, \quad t > 0 \end{aligned} \tag{13}$$

where θ_i is the initial soil moisture content, θ_s is the saturation moisture content, and r_o is the radius of the source.

If one starts with equation 5 rather than equation 7, the two-dimensional flow equation in polar coordinates is

$$C \frac{\partial h}{\partial t} = \frac{1}{r} \frac{\partial}{\partial r} \left(K r \frac{\partial h}{\partial r}\right) + \frac{1}{r^2} \frac{\partial}{\partial \varphi} \left(K \frac{\partial h}{\partial \varphi}\right) - \cos \varphi \frac{\partial K}{\partial r} + \frac{1}{r} \sin \varphi \frac{\partial h}{\partial \varphi} \tag{14}$$

with the initial and boundary conditions

$$\begin{aligned} h &= h_i, \quad r > 0, \quad t = 0 \\ h &= 0, \quad r = r_o, \quad t > 0 \\ h &= h_i, \quad r \to \infty, \quad t > 0 \quad . \end{aligned} \tag{15}$$

Determination of Transmission Coefficients

Both equation 12 and equation 14 are nonlinear. To achieve a numerical solution, the equations must be linearized at each time step by choosing values of the required transmission coefficients, D, K, and C, which can be assumed constant over a small region during a small-time increment. This requires knowing how the parameters vary with θ but does not necessarily require a functional relationship. Discrete values of the coefficients corresponding to certain values of θ may be used by interpolating between relatively closely spaced tabular values.

Equation 12 requires $K(\theta)$ and $D(\theta)$ relations but does not require the use of the water capacity, $C(\theta)$, unless water contents are to be converted to head values. For equation 14, $C(h)$ and $K(h)$ are required for solution. In either case, two coefficient relations are required; but as can be seen from equation 6, once two are known, the third can be calculated. Therefore, the choice of which two are measured depends on the accuracy and convenience of methods available for their determination.

Interest in a drying curve or a wetting curve will determine which method to use. For irrigation system design, the coefficients must be determined for the wetting case. For this study $C(\theta)$ and $D(\theta)$ were determined from experimental data and $K(\theta)$ was calculated.

Water capacity determination

The water capacity at a particular value of θ is the slope of the soil moisture characteristic--the curve relating capillary pressure head to moisture content for the side of the hysteresis loop which is of interest. The moisture characteristic is generally determined using pressure plate apparatus. Starting with saturated soil samples, pressure increments are applied step-wise until continued moisture content change with increased pressure is small. The soil is left at each pressure level until outflow ceases. The pressure and equilibrium moisture content at the end of each increment form one point on the

moisture characteristic curve. After completion of the desorption curve, incremental decreases in pressure provide data for the absorption curve by keeping the bottom of the plate in contact with water under low (near zero) pressure.

Klute (1967) described individual sample pressure cells which are convenient for determining both wetting and drying soil moisture characteristic curves. Similar cells were used in this study.

Diffusivity determination

While many methods have been developed for determining K and D functions, the majority of them are not applicable for obtaining absorption curves. Among the unsteady state methods for determining transmission coefficients are two similar methods which use data from flow into a horizontal column to determine $D(\theta)$. The first of these, developed by Bruce and Klute (1956), involves the use of data on the moisture content distribution along a horizontal column after infiltration has proceeded for some period of time. The second, suggested by Whisler, Klute and Peters (1968) requires data on the moisture content variation with time at a given point. Moisture content must be measured by nondestructive methods such as gamma absorption. Both methods make use of the Boltzmann transformation in the partial differential equation of diffusion for a horizontal column

$$\frac{\partial \theta}{\partial t} = \frac{\partial}{\partial x} \left(D \frac{\partial \theta}{\partial x} \right) \qquad (16)$$

where x is distance from a water source along a horizontal column. The Boltzmann transformation is given by

$$\lambda = xt^{-\frac{1}{2}} \tag{17}$$

where λ is a function of θ only. The use of this transformation assumes that water content is a single-valued function of h (or that soil is only wetting). Using the Boltzmann transformation in equation 16 leads to

$$-\frac{\lambda}{2}\frac{d\theta}{d\lambda} = \frac{d}{d\lambda}\left(D\frac{d\theta}{d\lambda}\right) \quad . \tag{18}$$

The use of the Boltzmann transformation converts the partial differential equation into an ordinary differential equation which can be integrated. Integrating and solving for D results in

$$D(\theta) = -\frac{1}{2}\left(\frac{d\lambda}{d\theta}\right)_{\theta_x}\int_{\theta_i}^{\theta_x}\lambda d\theta \tag{19}$$

where θ_x is the moisture content at any particular value of x and its use as a subscript indicates that the derivative is evaluated at $\theta = \theta_x$. Where the Bruce and Klute method is used and the moisture content determined along the column at a constant time, equation 19 can be expressed as

$$D(\theta) = -\frac{1}{2t}\left(\frac{dx}{d\theta}\right)_{\theta_x}\int_{\theta_i}^{\theta_x} x\, d\theta \tag{20}$$

by substituting $xt^{-\frac{1}{2}}$ for λ and recognizing that t is constant. Data on x versus θ are determined by sectioning a uniformly dense horizontal

soil column after infiltration advance has proceeded through most of the length of the column. The data can be used to evaluate $(\frac{dx}{d\theta})_{\theta_x}$ and the integral.

If the method of Whisler, Klute and Peters is used, x is constant and the moisture content variation with time must be measured. The equation for D can then be written

$$D(\theta) = \frac{1}{4}x^2 t^{-3/2}(\frac{dt}{d\theta})_t \int_{\theta_i}^{\theta_t} t^{-\frac{1}{2}} d\theta \quad . \tag{21}$$

Data on θ at various values of t throughout the infiltration process are used to evaluate $(\frac{dt}{d\theta})_t$ and the integral in equation 21.

Selim, Kirkham and Amemiya (1970) applied these two methods concurrently and found the results to be in agreement. Both methods were used on the same soil column in the current study. Results are given in Chapter V.

Solution of Equations

The goal in selecting a method for solving equation 12 or 14 was to choose a numerical procedure which would result in a rapid computer solution. To be of value for design, the computer program would have to be economical so that it could be used several times to test a range of transmission coefficients expected in a given field.

To completely describe the infiltration from a buried lateral, a solution of equation 12 or 14 for the flow in a plane perpendicular to the pipe would be required. Numerical solutions for equations similar

to these have been achieved by Rubin (1968), Brandt et. al. (1971), and Kilic (1973), using a procedure known as the alternating direction implicit procedure (ADIP). In each case, coordinate axes were chosen so that one axis was parallel to the direction of gravity. While the ADIP is a relatively efficient procedure for solving two-dimensional problems, for a grid system containing N x M points, it requires M - 1 solutions of a system of N - 1 simultaneous equations. This method was considered too time consuming to be a useful design tool and therefore was not programmed.

Allada and Quon (1966) discussed an alternating direction explicit procedure (ADEP) for solution of multi-dimensional problems which they indicated reduced the computer time required for solution of two-dimensional heat equations by a factor of about five as compared to the ADIP. The ADEP is stable for all time steps for the linear heat equation, but the author has been unable to use the method successfully to solve equation 12.

Since for design of subsurface irrigation systems the primary concern is predicting the distance the wetting front moves vertically and horizontally to determine proper depth and spacing for laterals, it was decided that possibly considering one direction at a time would be adequate rather than solving for the flow in the entire region. This idea simplifies the problem to solving a one-dimensional equation. The equation for one-dimensional radial flow can be deduced from equation 12

by setting derivatives in the angular direction equal to zero, leaving

$$\frac{\partial \theta}{\partial t} = \frac{1}{r} \frac{\partial}{\partial r} \left(D r \frac{\partial \theta}{\partial r} \right) - \cos \varphi \frac{\partial K}{\partial r} \qquad (22)$$

where $\cos \varphi = 1$ (ie $\varphi = 0$) vertically down from the source, $\cos \varphi = 0$ ($\varphi = 90^{o}$) along a horizontal axis through the source, and $\cos \varphi = -1$ ($\varphi = 180^{o}$) vertically up from the source.

Separate solutions are required for flow horizontally, vertically up, and vertically down from the source. The use of a one-dimensional solution early in the infiltration process is justified because as Philip (1969a) indicated, for a soil which is initially well below saturation, the flow is at first radially symmetric.

As time progresses and the gravitational influence on the flow becomes significant, one may wonder about the use of separate one-dimensional solutions. Some insight into the flow conditions can be seen by studying the flow net for steady flow from a buried source such as derived by Gilley and Allred (1972) from a theoretical solution of the flow equation. An example of flow lines and equal head lines is shown in Figure 1. The flow shown is for one-half the region between two sources where infinite flow regions are assumed above and below the source and no flow occurs across the right boundary. This flow situation is the opposite extreme from the radially symmetric flow at early flow stages. While steady flow is not approached in the situation studied here, Figure 1 illustrates the shape toward which flow lines will tend.

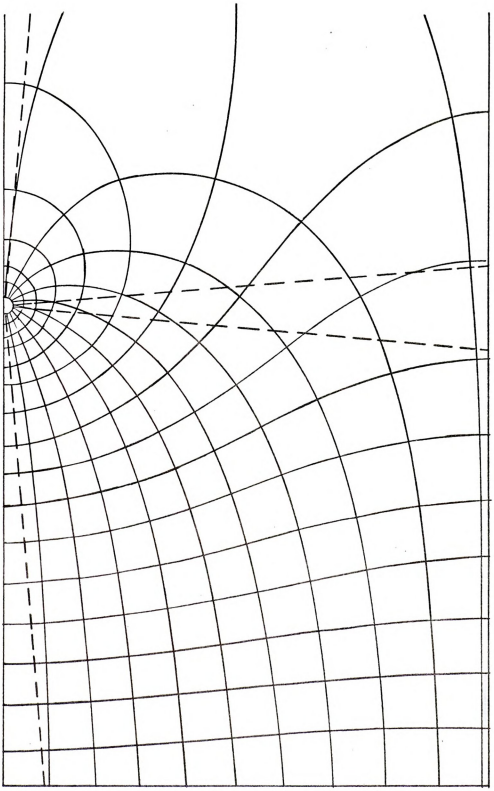

Figure 1. Radial Flow Wedges Superimposed on Flow Lines and Equal Head Lines for Steady Flow from Subsurface Source

The one-dimensional equation accounts for the effect of gravity on the driving potential in the radial direction but does not account for the bending of the flow lines caused by the effect of gravity on flow outside the axis-symmetric wedges shown dotted in Figure 1. If one considers a wedge symmetric about the vertical axis down from the source, the boundaries of the wedge are nearly parallel to the flow lines. The one-dimensional solution should closely approximate the actual flow situation vertically down, but the advance of the wetting front should be slightly underpredicted.

For the case of flow vertically up, the flow lines diverge from the boundaries of a radial flow wedge. Therefore, a one-dimensional analysis should predict a wetting front advance greater than that which would actually occur.

Using a one-dimensional solution to simulate flow in a radially bounded wedge symmetric about a horizontal axis through the source, one must assume that any flow which enters the wedge along flow lines from the region above is balanced by flow from the wedge to the region below. Obviously, purely radial flow occurs in such a horizontal wedge for only a short time after initiation of flow, but the total effect may closely resemble radial flow.

For design purposes, the model does not have to describe the physical flow with complete accuracy but should give a good indication of the dimension of the wetted region. Since the flow conditions during

infiltration from an intermittently operated subsurface lateral do not approach steady state flow, the use of one-dimensional solutions seemed worthy of investigation.

Equation 22 can be written in terms of the degree of soil saturation by using the definition

$$\theta = \eta S \tag{23}$$

where η is the porosity of the soil and S is the degree of saturation or the fraction of total pore volume which is filled with water. Since η is a constant for homogeneous soil, using equation 23 in equation 22 yields

$$\frac{\partial S}{\partial t} = \frac{1}{r}\frac{\partial}{\partial r}\left(D\, r \frac{\partial S}{\partial r}\right) - \frac{\cos\varphi}{\eta}\frac{\partial K}{\partial r} \quad . \tag{24}$$

In order to achieve a numerical solution, equation 24 must be expressed in finite difference form. Remson, Hornberger and Molz (1971) pointed out that finite difference representations should be convergent and unconditionally stable, meaning that their solution should converge to the solution of the differential equation as finite difference approximations approach zero and that errors should not grow with time. Solutions should have relatively small truncation errors and should be easy to compute. They further stated that equations such as equation 24 can be solved using a predictor-corrector technique based on modifications of implicit difference techniques. They suggested the use of a predictor-corrector proposed by Douglas and Jones (1963) which uses a

predictor based on an implicit finite difference representation of the equation and a corrector based on the Crank-Nicholson procedure. This method satisfies the convergence and stability criteria and has truncation errors of second order magnitude. Fitzsimmons (1972) used this method to simulate one-dimensional unsaturated radially symmetric flow in a horizontal plane.

The predictor form for equation 24 written for flow downward is

$$r_i \frac{S_{i,j+\frac{1}{2}} - S_{i,j}}{\Delta t/2} = D_{i+\frac{1}{2},j}\, r_{i+\frac{1}{2}} \left(\frac{S_{i+1,j+\frac{1}{2}} - S_{i,j+\frac{1}{2}}}{\Delta r^2}\right) - D_{i-\frac{1}{2},j}\, r_{i-\frac{1}{2}} \left(\frac{S_{i,j+\frac{1}{2}} - S_{i-1,j+\frac{1}{2}}}{\Delta r^2}\right) - \frac{r_i}{\eta} \left(\frac{K_{i+\frac{1}{2},j} - K_{i-\frac{1}{2},j}}{\Delta r}\right) \qquad (25)$$

where the i subscripts refer to the location in the r direction and the j subscripts refer to the time at which a variable is evaluated. The predictor contains values of saturation at a known time and at one-half time interval forward. This is an implicit expression because the saturation values on the right side of the equation are evaluated at the unknown time level, $j+\frac{1}{2}$. To solve the expression, it is necessary to write this equation for each of the grid points in the r direction and then solve the system of simultaneous equations which result. The corrector, which uses values of $S_{i,j+\frac{1}{2}}$ to evaluate transmission coefficients, is used to advance the solution to the next full time increment. The corrector for equation 24 can be expressed as

$$r_i \frac{S_{i,j+1} - S_{i,j}}{\Delta t} = D_{i+\frac{1}{2},j+\frac{1}{2}} r_{i+\frac{1}{2}} \left(\frac{S_{i+1,j} - S_{i,j}}{2\Delta r^2} + \frac{S_{i+1,j+1} - S_{i,j+1}}{2\Delta r^2} \right)$$

$$- D_{i-\frac{1}{2},j+\frac{1}{2}} r_{i-\frac{1}{2}} \left(\frac{S_{i,j} - S_{i-1,j}}{2\Delta r^2} + \frac{S_{i,j+1} - S_{i-1,j+1}}{2\Delta r^2} \right)$$

$$- \frac{r_i}{\eta} \left(\frac{K_{i+\frac{1}{2},j+\frac{1}{2}} - K_{i-\frac{1}{2},j+\frac{1}{2}}}{\Delta r} \right) \quad . \tag{26}$$

To move the solution forward one full time step, it is necessary to solve two systems of simultaneous equations, one based on the predictor and a second based on the corrector. The solution for the predictor will be illustrated. First, multiplying through equation 25 by $\frac{\Delta t}{2}$ and collecting like S terms results in an equation of the form

$$A_i S_{i-1,j+\frac{1}{2}} + B_i S_{i,j+\frac{1}{2}} + C_i S_{i+1,j+\frac{1}{2}} = R_i$$

where

$$\begin{aligned}
A_i &= - \frac{\Delta t}{2\Delta r^2} r_{i-\frac{1}{2}} D_{i-\frac{1}{2},j} \quad , \\
B_i &= r_i + \frac{\Delta t}{2\Delta r^2} \left(r_{i-\frac{1}{2}} D_{i-\frac{1}{2},j} + r_{i+\frac{1}{2}} D_{i+\frac{1}{2},j} \right) \quad , \\
C_i &= - \frac{\Delta t}{2\Delta r^2} r_{i+\frac{1}{2}} D_{i+\frac{1}{2},j} \quad , \\
R_i &= r_i S_{i,j} - \frac{\Delta t r_i}{2\eta\Delta r} \left(K_{i+\frac{1}{2},j} - K_{i-\frac{1}{2},j} \right) \quad .
\end{aligned} \tag{27}$$

Writing equation 27 for each of N - 1 grid points in the r direction forms a set of N - 1 simultaneous equations containing N - 1 unknowns. The complete set of equations can be illustrated by

$$
\begin{aligned}
B_1S_1 + C_1S_2 &= R_1 - A_1S_0 \\
A_2S_1 + B_2S_2 + C_2S_3 &= R_2 \\
A_3S_2 + B_3S_4 + C_3S_5 &= R_3 \\
&\vdots \\
A_{I-1}S_{I-2} + B_{I-1}S_{I-1} + C_{I-1}S_I &= R_{I-1} \\
A_IS_{I-1} + B_IS_I &= R_I - C_IS_{I+1}
\end{aligned}
\qquad (28)
$$

where $I = N - 1$ and the first equation is for the first grid point beyond the source boundary and the last equation is the grid point at the outside boundary of the flow region. Equations 28 form a tridiagonal matrix which can be solved by a procedure known as Gaussian elimination. Ozisik (1968) has given a summary for using the Gaussian elimination procedure as follows:

1. A suitable multiple of the first equation in system 28 is subtracted from the second equation to eliminate S_1.

2. A suitable multiple of the new second equation is subtracted from the third equation to eliminate S_2, and the procedure is continued.

3. A suitable multiple of the new equation before the final one is subtracted from the final equation to eliminate S_{I-1}.

4. The unknown S_I is immediately evaluated from the new final equation.

5. The remaining unknowns--S_{I-1}, S_{I-2}, . . . , S_2S_1--are evaluated by substitution in the reverse order.

After performing the first three steps, the resulting new equations are

$$
\begin{aligned}
S_1 + E_1 S_2 &= F_1 \\
S_2 + E_2 S_3 &= F_2 \\
S_3 + E_3 S_4 &= F_3 \\
&\vdots \\
S_{I-1} + E_{I-1} S_I &= F_{I-1} \\
S_I &= F_I \quad .
\end{aligned}
$$

Ozisik also has given recurrsion relations for forming the coefficients in equations 29 from coefficients in equations 28 as follows:

$$
\begin{aligned}
E_1 &= \frac{C_1}{B_1}, \qquad F_1 = \frac{R_1}{B_1} \\
E_i &= \frac{C_i}{B_i - A_i E_{i-1}}, \qquad F_i = \frac{R_i - A_i F_{i-1}}{B_i - A_i E_{i-1}} \qquad i > 1
\end{aligned}
\tag{30}
$$

The corrector is set up and solved in basically the same way as the predictor.

The solutions were set up and performed using a Fortran IV program on the Michigan State University CDC 6500 computer. Results of the solutions are discussed in Chapter VI.

IV. EXPERIMENTAL PROCEDURES

The primary goal of the experimental aspect of this study was to run laboratory tests of infiltration from a buried porous pipe simulating subsurface irrigation. Data were collected to characterize the growth of the wetted soil region around a subsurface irrigation source under a given set of conditions. The advance of the visual wetting front, the moisture content distribution in each of three major directions from the source (vertically up, vertically down, and horizontally), the inflow rate, and the development of the saturated zone around the source were recorded.

Selection of Moisture Measurement Technique

A nondestructive process for measurement of soil moisture content during infiltration was desired, and several alternatives were explored. Infrared photography using film sensitive in the near infrared (less than 0.9 micron) was considered as a possibility for instantaneously determining the moisture content throughout the chamber photographically. Sewell, Allen and Pile (1971) found that the use of infrared photography had potential for determining the moisture content of soils.

Six boxes 6 x 6 x 3 in. were built and packed with soil. They were brought to different equilibrium moisture contents, placed so all would

show in one frame, and photographed with various combinations of infrared films and filters. A film densitometer was used to determine emulsion density differences on the exposed film resulting from differences in both visual and infrared light reflectance by soil samples of different moisture content.

Figure 2 shows a typical relationship between infrared film density and moisture content. In the low moisture content range, the infrared reflectance as measured by film density is not greatly affected by moisture. At higher moisture contents, the film density decreased, probably as a result of sufficient moisture attached to soil particles to reflect light rays rather than absorb them. Low sensitivity at low moisture contents and the double valued relation at higher moisture contents caused the author to reject infrared photography as a means of moisture content determination for laboratory chambers.

The field of choices was then narrowed to various point measurement techniques. Moisture content can be measured indirectly at a point with tensiometers, thermocouple psychrometers, heated porous blocks, or gamma ray absorption. Tensiometers have limitations in the dry moisture content range, and thermocouple psychrometers are not accurate near saturation. Heated porous blocks described by Phene, Hoffman and Rawlins (1971) are difficult to calibrate and are expensive.

The gamma ray system was chosen and its use had a bearing on the configuration of the soil chamber developed. Using gamma ray requires

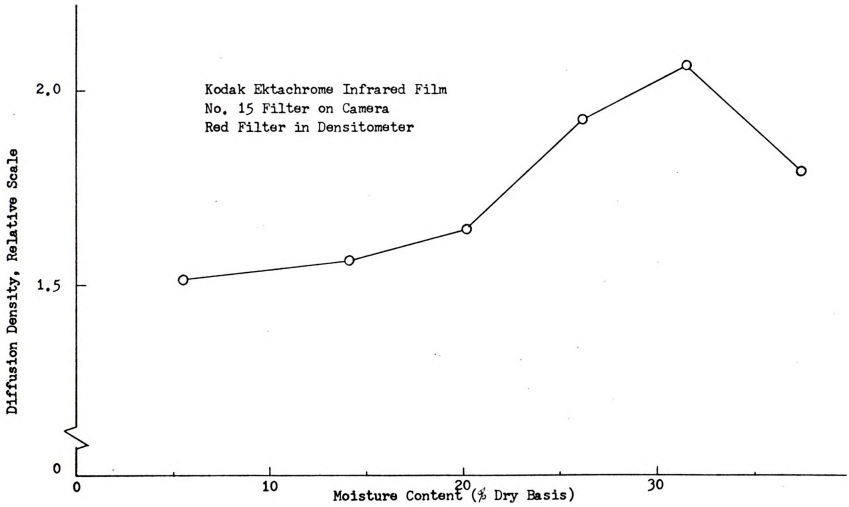

Figure 2. Relation Between Film Density and Soil Moisture Content of Warsaw Loam

a radiation source on one side of the chamber and a radiation detector on the other side so that a beam of gamma radiation can be passed through the chamber at right angles to its confining walls. Details of the method and equipment used are described later in this chapter.

Description of Soil Chamber

Before fabricating the primary chamber, small boxes 12 x 12 x 6 in. deep and 12 x 12 x 3 1/4 in. deep were built from acrylic plastic, and short-time infiltration trials were run to determine edge effects and methods of soil placement for larger chamber tests. A section of porous pipe was placed in the center of the 12-in. square face. Various methods of soil placement were tested to discover a way of packing soil uniformly. Placing approximately 1-in. thick layers of air dry soil using an elongated funnel followed by careful tamping resulted in sufficiently uniform soil density.

The soil in the small chambers was partially wetted from the central pipe and then the dry soil around the wetted region removed to determine whether the advance of the wetting front was affected by the interface between the chamber wall and the soil. No wall effects were found.

In designing a large chamber to run full-scale simulations of subsurface irrigation, two constraints were to be satisfied. First, it had to be possible to scan at least half of the chamber with a gamma ray system used to measure soil moisture content; and secondly, a means

had to be provided for drying the soil in the chamber relatively easily and rapidly so that several tests could be run with one soil packing. One packing would eliminate density variations which would unavoidably occur if the chamber had to be repacked between tests. Using the same soil packing would also eliminate the laborious and time-consuming task of repacking a large soil chamber in a uniform manner.

Tests with the small chambers substantiated the feasibility of removing an acrylic face from one side of the soil chamber and drying the chamber with heated air in a period of a few days if the minimum dimension could be placed perpendicular to the flow of heated air. Coating the removable face with a silicone coating[1] made it easy to remove from moist soil with only a few soil particles stuck to the acrylic sheet.

Following the tests with small chambers, a large chamber with inside dimensions of 66 x 47 x 3 1/4 in. was fabricated for use in testing infiltration during subsurface irrigation. Figure 3 is a photograph of the large experimental chamber, which consists of a 3/4-in. marine plywood back and nominal 1-in. pine sides and bottom. The wooden interior of the soil chamber was painted with three coats of epoxy marine paint to prevent moisture absorption by the wooden components. The plywood back was supported by 3-in. channel iron on

---

[1] Dow Corning "Pan Shield," a silicone coating marketed for cooking utensils.

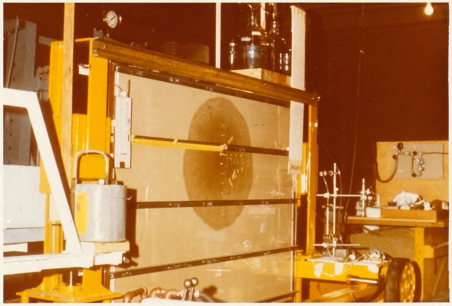

Figure 3. Soil Chamber

approximately 12-in. centers which were welded to 4-in. channel iron side supports to provide a rigid frame.

To facilitate removing the acrylic face and drying the soil, the chamber was suspended so that after an experimental run, the chamber could be rotated 90 degrees, placing the removable face in a horizontal plane. The chamber support frame was built stoutly so that essentially no deflection would occur when the chamber was rotated onto its back for removal of the face and soil drying. If the chamber framework were to sag, cracks would form in the soil pack and would be exaggerated during the drying process. Significant cracks would render the soil pack essentially useless for subsequent experiments. Figure 4 shows the soil chamber in the drying position.

The front of the chamber was supported by spacers fabricated from 1/4-in. pipe placed on approximately a 12-in. grid throughout the chamber. Figure 5 is a diagram of a typical spacer through the soil chamber. The ends of the spacers were enlarged to bear against both the plywood back and the acrylic face. A nut was welded to the front end of each spacer and a 1/4 x 5-in. bolt was threaded through the spacer with its head bearing on the channel iron support on the back of the chamber. This arrangement held the spacer rigidly in place and provided a threaded stud on the front of the chamber for securing the removable face. Supports made from 1 1/4 x 1/8-in. angle iron were used lengthwise along the front of the chamber on the outside of the acrylic face to prevent excessive deflection between spacers.

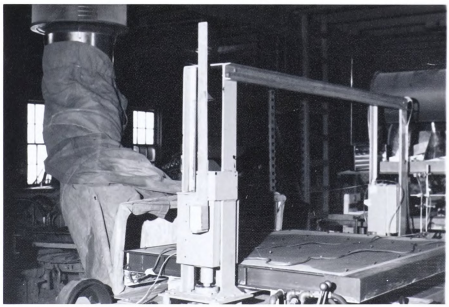

Figure 4. Soil Chamber in Drying Position

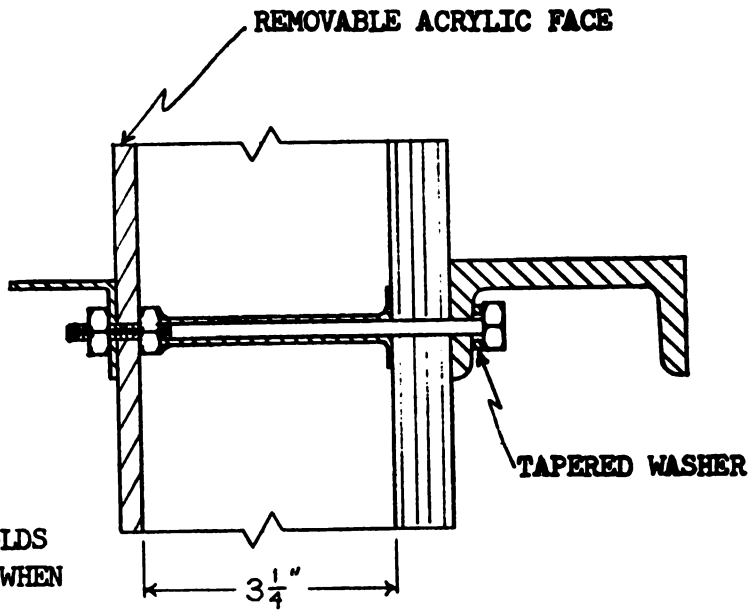

Figure 5. Cross Section of Spacer Used on 1-Ft. Grid Throughout Soil Chamber

To prevent water from ponding in the bottom of the soil chamber, a drainage system was installed. A 60-in. piece of 3/4-in. plastic pipe perforated with 1/8-in. drilled holes every 4 in. was wrapped with fiberglass drain filter material and mounted 1 in. above the bottom of the soil chamber. Outlets at both ends of the drainage pipe led through the back of the chamber.

The chamber was supported on two 3/4-in. pins, one at each end. These were welded to plates which were bolted to the chamber so that the pins could be adjusted to pass through the calculated center of mass of the chamber. The pins were supported in cradles which were fastened to brackets on 4-in. hydraulic cylinders. These cylinders raised and lowered the chamber enough for scanning most of the vertical expanse of the chamber with the gamma ray moisture sensing system. A heavy steel guide supported the soil chamber mounting brackets on top of the cylinder rods and prevented bending in the rods as the cylinders were raised and lowered.

The supporting cylinders were mounted on a wheeled frame which ran on a level track and provided for horizontal movement of the soil chamber through the gamma ray beam. The wheeled frame and track were part of a soil bin tillage testing facility in the Agricultural Engineering Department. This facility had a central frame spanning the track for positioning tillage tools. The central frame was mounted on a vertical pole which provided for 23 in. of vertical movement of the entire framework.

The gamma ray source and sensor were mounted on a pair of parallel trusses which were cantilevered from the existing tillage tool frame far enough to reach the center of the soil chamber. To provide accurate repeatable placement of the gamma beam with respect to the soil chamber both horizontally and vertically, scales were fastened to the track and to the vertical pole, and indices were mounted on the wheeled frame and on the movable frame on which the moisture sensing system was mounted. Repeat placement of a given point of the soil chamber in the beam was within ± 0.5 mm. The wheeled frame was moved laterally by hand, and vertical movement of the moisture sensing system was provided by a reversible 1 horsepower electric motor driving a gear reduction and in turn a slip clutch which turned on a 3/4-in. threaded shaft fastened to the movable frame. The reduction system provided a vertical travel speed of about 7.5 in./min. A reversing switch mounted at the support pole allowed vertical adjustment of the moisture sensing system.

A total vertical scan capability of 40 in. was provided by a combination of the 23-in. travel of the source and sensor mounted on the vertical pole and 17 in. of soil chamber movement provided by the hydraulic cylinders. The sensing system was positioned so that the upper limit of the vertical scan capability was 2 in. below the soil surface, making the lower limit approximately 5 in. above the bottom of the soil chamber.

Moisture and Density Measurement by Gamma Ray

Theory of the method

The use of the gamma ray attenuation technique for measurement of soil moisture content and/or soil density is well established. Gardner (1965) summarized the principles, special apparatus, and procedure used in the application of gamma ray for soil measurements. The method is based on the principle that as radiation passes through a uniform substance, there is a constant fractional decrease in radiation per unit thickness of absorber, and the fractional decrease depends on the density and absorption characteristics of the material acting as an absorber. In equation form, this can be expressed as

$$I = I_o \exp(-\mu\rho s) \tag{31}$$

where I is the radiation intensity after passing through the absorber, I_o is the intensity striking the absorber, μ is the mass absorption coefficient of the absorbing substance, ρ is the density, and s is the length of absorber.

Vachaud (undated) indicates that for this equation to hold, the relation should be defined by a single energy peak and diffused photons should be eliminated. This can be accomplished by the proper selection of a source and by careful collimation of the radiation both as it leaves the source and approaches the sensor. Incident photons can be converted to electronic pulses by a NaI crystal associated with a photomultiplier. Upon bombardment by gamma photons, luminous photons are

liberated by the crystal and excite the photo cathode of the photo-multiplier. Connection to a suitable scaler completes the conversion of incident energy to digital counts. Fluctuation in count rate through a constant medium results from the random nature of radiation emission from the source. While there is a definite average rate of emission from a gamma source, the nuclear disintegration producing the radiation occurs in a random manner. Lapp and Andrews (1954) indicate that individual count observations have a Poisson distribution and that an estimate of the standard deviation of a single observation of N counts is

$$\sigma = \sqrt{N} \quad . \tag{32}$$

Equation 1 can be expressed in terms of counts as

$$N = N_o \exp(-\mu\rho s) \tag{33}$$

where N and N_o stand for count rates after passing an absorber and incident upon the absorber, respectively. For a soil-water system confined in a container so that an incident gamma beam must pass through two container walls, equation 33 can be expressed as

$$N = N_o \exp[-(\mu_s\rho_s + \mu_w\rho_w\theta)\, s - 2\mu_c\rho_c s_c] \tag{34}$$

where the subscripts s, w, and c indicate soil, water, and container, respectively. The container terms can be eliminated by replacing N_o by the counts through an empty chamber, resulting in

$$N = N_c \exp[-(\mu_s\rho_s + \mu_w\rho_w\theta)\, s] \quad . \tag{35}$$

If the chamber is packed with air dry soil, then equation 35 can be expressed as

$$N_{ad} = N_c \exp\left[-(\mu_s\rho_s + \mu_w\rho_w\theta_{ad})\, s\right] \tag{36}$$

where the subscript ad on N_{ad} and θ_{ad} stands for air dry moisture content.

Solving for the density, it is seen that to compute soil density, one must take counts through an empty chamber at a given point followed by counts through air dry soil in the chamber at that point.

$$\rho_s = \frac{-\mu_w\theta_{ad}}{\mu_s} - \frac{\ln(N_{ad}/N_c)}{\mu_s s} \tag{37}$$

When the density of soil at a point is known as well as the count rate through dry soil at that point, the moisture content after wetting can be calculated by using the reference count in equation 35 as N_{ad} instead of N_c and solving for the moisture content, θ. This results in

$$\theta = \theta_{ad} - \frac{\ln(N_m/N_{ad})}{\mu_w s} \tag{38}$$

where N_m is the count rate through moist soil. Use of equation 38 assumes that the soil density remains constant during moisture content determinations.

During a short time as each count builds up on the photomultiplier of the detector, the equipment is insensitive to incoming radiation. This time period is called the dead time or the resolution time of the instrument. If a count ratio such as N_{ad}/N_c in equation 37 or N_m/N_{ad} in equation 38 is not close to 1, it may be necessary to make an

adjustment for the dead time, t_d, as follows

$$\left(\frac{N_{ad}}{N_c}\right)_{adj} = \frac{N_{ad}}{N_c} \cdot \frac{T_t - t_d N_c}{T_t - t_d N_{ad}} \qquad (39)$$

where T_t is the counting time used to obtain N_{ad} and N_c.

Corey, Peterson and Wakart (1971) discuss the use of two gamma ray sources with widely separated energy peaks for the determination of moisture content and density simultaneously. Gardner, Campbell and Calissendorff (1972) discuss the choice of sources for dual gamma energy density and water content measurements and evaluate in detail errors associated with the method. For this study dual sources were not available. A single source was used, forcing the assumption of constant density during moisture content determinations.

Description of equipment used

The moisture content determination equipment used is described in detail by Qazi (1970). The source consisted of a 100 mc. capsule of ^{137}Cs placed in a lead shield providing a minimum of 10 cm. shielding around the source in all directions. A collimation plug was inserted in one side of the shield and drilled with a 6 mm. hole. The source was mounted on a bolt so that alignment of the source on the collimated plug could be achieved. The detector used was a modified Nuclear Chicago Model DS-100 scintillation detector with a 1 1/2-in. NaI crystal connected to a photomultiplier and preamplifier. It had a resolution time of 1.5 microseconds/count. The detector was connected to a

Nuclear Chicago Model 8725 analyzer/scaler equipped with a 6-decade scaler, electronic timer, a single-channel gamma radiation analyzer, and a scintillation detector high voltage power supply. The scaler contained a discriminator which could be set to reject pulses resulting from gamma energies below a certain level and a window which could be set to reject energies above a certain level. The discriminator was calibrated so that a base level setting of 6.00 volts corresponded to a gamma energy level of 0.600 Mev. and all energy levels below that were rejected. Since ^{137}Cs has a peak at 0.661 Mev. and its energy spectrum drops rapidly beyond that, a base discriminator setting of 0.600 and a mode setting corresponding to an infinite window was used so that all energy levels above 0.600 Mev. were sensed in this study. A high voltage adjustment on the power supply to the scintillation crystal was provided. Occasional adjustment of this high voltage was necessary to obtain a peak count through an aluminum block used as a standard.

At the onset of the study the detector was expected to be temperature sensitive and to require some temperature control. Kriz (1969) published information on temperature calibration of a Hewlett-Packard Company scintillation detector. With this detector he found that as temperatures increased above approximately 76°F, it was necessary to increase the voltage supply to the detector to maintain the same peak count rate, but the voltage increase required was predictable. Reginato and Stout (1970), using Hamner Electronics equipment intended

for field use, found that the voltage setting required to attain a peak count rate decreased as temperature increased from 10 to 30°C and that the peak count attained increased as temperature increased.

Therefore, the temperature effect on the DS-100 detector planned for use was investigated. The probe and source were placed in an environmentally controlled chamber connected to an Aminico Aire unit capable of producing a wide range of temperature and humidity conditions. The effect of temperature seemed to be slight both on the voltage required to produce a peak count rate and on the peak count rate itself as temperature varied between 57.5 and 60°F. Analysis indicated that temperature could not be considered a useful predictor of count rate. However, when the equipment was moved to an uninsulated building to be used for large chamber tests, it showed marked drifts in count rate which were related to temperature fluctuations in the building. Insulating and air conditioning the detector as suggested by Vachaud (undated) did not solve the problem. It was necessary to insulate and keep the scaler at a constant temperature to stabilize the count rate as temperatures within the building fluctuated. Two-inch thick styrofoam sheets were used to build an insulated chamber surrounding the scaler and the detector. Both were ventillated with constant temperature air from an Aminico Aire unit. The temperature within the insulated scaler chamber was kept at 70 ± 1°F for all tests.

Determination of mass absorption coefficients

Before equations 37 and 38 could be used, it was necessary to determine the absorption coefficients for soil and water. Gardner (1965) pointed out that while the absorption coefficient for water can be obtained from tables, it is best to empirically determine the coefficient for the geometry and electronic discrimination system to be used for the test. Considering equation 34 for water and container only and letting the reference count be the count through the empty container gives

$$N_w = N_c \exp(\mu_w \rho_w \theta S) \tag{40}$$

where the count N_w is the count taken through a container filled with water only. Solving for the absorption coefficient and noting that for a water filled container θ is unity gives

$$\mu_w = \frac{\ln(N_w/N_c)}{S\rho_w} \tag{41}$$

where ρ_w is in gm/cc, S is in cm, and therefore μ_w is in cm^2/gm.

For this study four acrylic boxes 2.82 x 4.80 x 5 cm. were used in the determination of μ_w. The four boxes were placed adjacent to one another and positioned in the beam so that the center of the beam passed through the center of the boxes traversing the 2.82 cm. dimension. The coefficient was determined for different energy bands by varying the discriminator setting on the gamma ray equipment. Two 3-minute counts were taken through the center of the four empty boxes. Starting with the box nearest the source, one box was filled with

water and two more 3-minute counts were taken. Another box was filled and two more counts taken until all four boxes were filled. Results of these measurements for various energy levels are shown in Figure 7, where the absorption coefficient is plotted against the water thickness through which the beam traversed. The attenuation coefficient varied with the water thickness and also varied rather widely with the energy level setting on the discriminator. Qazi (1970) used the same equipment and found also that the mass absorption coefficient for water depended on the thickness of water in the beam.

Stroosnijder and deSwart (1973) reported that for nonideal collimation, the position of the water along the beam while taking data for determining the absorption coefficient affects the result.

The data for the .656-.666 Mev. and the .611-.711 Mev. curves in Figure 7 were taken during preliminary work, but the curve for all energies above .600 Mev. represents data taken with the gamma ray equipment in place and collimated for the infiltration experiments. For all three curves, the containers were filled with water in the same order. The position of the containers in the beam was not carefully controlled, so the shape of the curves may be related to the positioning of the containers in the beam.

The .600 Mev. curve was determined with the containers at the same location in the beam as that occupied by the soil chamber when it was in place. Therefore, a μ_w of 0.0825 was used for moisture content

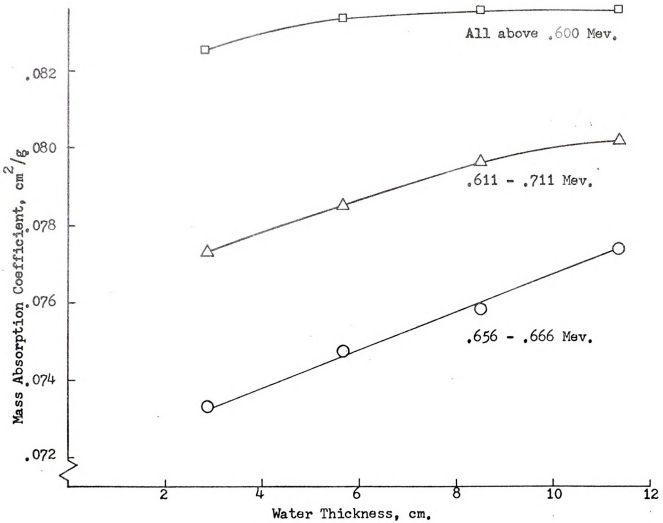

Figure 7. Variation of Mass Absorption Coefficient for Water vs. Thickness of Distilled Water in Beam for Different Energy Ranges

calculations for most of this study because the discriminator setting used was 0.600 Mev. and the maximum water thickness expected in the path of the beam was approximately 2.8 cm.

The soil absorption coefficient can be determined in similar fashion using oven dry soil or soil at a known uniform initial moisture content such as air dry. Equation 37 can be solved for μ_s, requiring first the determination of counts through an empty container and then through the soil filled container.

The mass absorption coefficient for soil was determined using a 6 x 6 x 3-in. acrylic box which was packed with soil in a manner similar to that used in packing the large chamber for the study. Prior to filling with soil, two 2-minute counts were taken at each of nine locations through the chamber walls. These points were on a 1 1/2 x 1 1/2-in. grid centered on the 6 x 6-in. side of the box. After packing, accurate measurements of the box's thickness at each of the counting locations was made with an outside micrometer. The wall thickness, also determined by micrometer, was subtracted from the outside dimension to get the length of soil traversed by the beam at each point. Two 2-minute counts were then taken at each of the nine points. The average bulk density in the box was determined by weight. Average counts, weights, and soil thickness values at the nine points were used to compute the average μ_s from equation 37 including a dead time correction. The mean and standard error were found to be 0.07767 ± 0.00037.

The four-box procedure used for μ_w determinations was also tried for μ_s determinations, but the increase in the absorption coefficient with increasing thickness which occurred for water did not occur for soil.

Filling the Soil Chamber

The large soil chamber was packed in the vertical position with the acrylic face in place. An elongated funnel with a foot valve was used to gently lower the soil into position. A 9-in. funnel was extended using a 4-ft. length of 3/4-in. plastic tubing. A length of 1/4-in. pipe was passed through guides fastened to the 3/4-in. plastic tubing, and a piece of flat steel welded to the end of the pipe could be slipped across the end of the tubing by rotating the shaft formed by the pipe. As the chamber was filled, the plastic tubing was periodically shortened to keep the funnel opening at a convenient working height. The soil was placed in 1-in. layers and each layer tamped in place by approximately three blows per square in. from a 3/4-in. square steel rod fastened to a 30-in. handle.

The funnel and tube were kept full of soil so that each successive layer of soil could be gently lowered into the chamber without particle size separation. The foot valve was closed while moving the funnel into and out of the chamber. The tamper was raised approximately 1 in. above the soil and lowered with a force of approximately 5 pounds.

Prior to filling the empty chamber, 2-minute gamma ray counts were taken at each point on a 4-in. grid over one-half of the chamber. After filling, the chamber was again scanned taking 2-minute counts at each point in the 4-in. grid. The thickness of the soil at each of the grid points was carefully determined by measuring the distance from a fixed point on the source shield to the front side of the chamber and from a fixed point on the sensor to the back side of the chamber with inside micrometers. Knowing the distance between the fixed points gave an accurate measure of the outside dimensions of the chamber at each grid point. The thickness of the acrylic face and plywood back were then subtracted from this outside dimension to get the inside dimension at each grid point. These data were used to compute the soil density distribution shown in Figure 8. The mean density and standard error for all grid points shown are 1.6801 gm/cc. ± 0.0033. If one deletes the grid points along the left boundary and along the upper surface, which are obviously in regions of lesser density, the mean density and standard error are 1.6897 gm/cc. ± 0.0029.

Infiltration Experiments

Experiments were conducted to study the infiltration from a buried porous pipe into soil at an initially uniform moisture content. An interior source pressure of 3 psi (6.1 in. Hg) was kept as constant as possible but occasionally varied slightly due to plugging of the filter used to remove substances which would otherwise plug the porous pipe.

Horizontal Distance from Source - Inches

Vertical Distance from Source - Inches	32	28	24	20	16	12	8	4	0
12	1.643	1.632	1.633	1.634	1.626	1.621	1.630	1.632	1.646
8	1.659	1.707	1.729	1.693	1.751	1.729	1.726	1.700	1.716
4	1.636	1.717	1.702	1.702	1.719	1.712	1.731	1.713	1.725
0	1.651	1.715	1.679	1.725	1.714	1.654	1.677	1.690	. source
- 4	1.663	1.711	1.708	1.704	1.712	1.688	1.724	1.670	1.717
- 8	1.659	1.688	1.686	1.726	1.681	1.660	1.699	1.674	1.623
-12	1.655	1.670	1.650	1.662	1.675	1.654	1.662	1.676	1.653
-16	1.650	1.701	1.687	1.710	1.654	1.691	1.688	1.670	1.681
-20	1.571	1.650	1.658	1.672	1.647	1.660	1.667	1.644	1.653
-24	1.636	1.678	1.673	1.665	1.704	1.672	1.678	1.672	1.702
-28		1.710	1.697	1.704	1.726	1.695	1.702	1.674	1.704

Figure 8. Density Distribution Over 4-Inch Square Grid Covering Left Half of Soil Chamber

The pressure control system consisted of a pair of interconnected Marriotte bottles mounted on top of the chamber and pressurized by nitrogen from a bottled gas supply. A pressure regulator was used to maintain just over 3 psi at the reference level in the bottles. The pressure in the moisture source was monitored by a mercury manometer which was connected to the water supply line just as it went into the porous pipe. A sliding scale on the manometer made it possible to read the source pressure to ± 0.02 in. Hg.

Water from the supply bottles passed through a 0.45 micron filter and a ball-type flow meter prior to entering the source. In addition to the main filter, a by-pass filter was mounted in parallel so that if the main filter started to plug, it could be clamped off and the by-pass filter used while a new filter membrane was installed in the main filter. As the main filter started to plug and the head loss increased slightly, a constant pressure at the source could be maintained by increasing the pressure to the supply bottles with the gas regulator. Before any test was run, phenol was added to distilled water to make a 0.1 percent phenol concentration, and the water was prefiltered to decrease the effect of pressure change due to filter plugging during a test. Two infiltration-drying cycles were made to settle the soil before any data were taken for analysis. Prior to each test, moisture content measurements using gamma ray radiation were made at 1-in. intervals along one horizontal and both vertical axes through the center of the source.

Before starting the flow to begin each test, water lines were completely filled with water and then clamped off and connected to the porous pipe embedded in the chamber. As the test was started, flow rate and pressure at the source were carefully monitored and data taken every few minutes on the rate of advance of the visual wetting front. After infiltration had run 30 minutes, 1 hour, 2 hours, 4 hours, and approximately every 4 hours thereafter, the locations of the wetting front were traced on the transparent face of the chamber and later photographed and transferred to tracing paper for future reference. In all the runs the wetted region remained symmetric about a vertical axis, indicating that the practice of scanning only the left half of the wetted region was adequate.

During each run the major axes were scanned 3 to 4 times with the gamma ray apparatus to determine the moisture content distribution. Scanning consisted of taking a 30-second count at 1-in. increments, starting 1/2 inch from the center of the source and proceeding past the wetting front. Near the wetting front, counts were sometimes taken at 1/2-in. intervals and a count was generally taken 1/2 in. from the source center. The chamber on the hydraulic cylinders was left in its lowest position while scanning horizontally and vertically up and was raised to its highest position to complete the vertically down scan after the lowest possible position had been reached with the cylinders down.

Before, after, and several times during each scan, counts were taken through an aluminum block used as a standard to establish a reference count for that scan. From time to time the reference count varied, so a ratio of the reference counts taken when the chamber had been scanned at air dry moisture content over the reference count taken during a given scan was used to correct counts. Using this ratio in equation 38 and including a dead time correction gives

$$\theta = \theta_{ad} - \frac{\ln\left(\frac{N_m}{N_{ad}} \cdot \frac{N_{oad}}{N_{om}} \cdot \frac{T_t - t_d N_{ad}}{T_t - t_d N_n}\right)}{\mu_w S} \qquad (42)$$

where N_{oad} is the count through the aluminum standard when counting air dry soil and N_{om} is the aluminum count during a scan of moist soil.

The duration of each test ranged from 20 to 24 hours. For the purpose of taking data, a test was considered complete when the wetting front reached either the soil surface or the bottom of the chamber, whichever occurred first. However, the water was allowed to continue to run until the wetting front had proceeded well beyond the region which would be of interest in the next test so that any salts which were being moved with the water would not affect the next run.

After the water was shut off at the completion of each test, several days elapsed to allow the moisture to redistribute and partially equalize the moisture content distribution. This was done to be sure that when drying was started, the region of most interest, i.e. the region around the source, would dry at a relatively uniform rate and a

nearly constant moisture content would result after drying. Following redistribution, a cover was clamped on the top of the soil chamber, all hardware related to the water supply system was removed, and the chamber was rotated to a horizontal position. The acrylic face was then removed, heat cables on the back of the chamber energized, and heated air flow over the exposed soil face started. While no measurements of moisture content were possible during the drying process, the disappearance of moisture from the soil surface looked uniform over the chamber. This indication of uniform drying was verified by gamma ray scans after drying which showed no excessive moisture content variation along the major axes.

Drying time varied from 8 to 48 hours, depending on the desired final moisture content. The heat cable and the hot air passing over the soil caused the soil temperature to exceed $140^{\circ}F$ after several hours of drying. After the drying system was disconnected, the chamber was allowed to come to temperature equilibrium prior to replacing the acrylic face. After the face was installed, at least five more days elapsed prior to running the next test.

V. SOIL PROPERTIES

Physical Properties

The soil chosen for use in this study was a mixture of Fox loam B horizon from the Kellogg Farm and a fine sand from near the pistol range located on a hill just east of the Michigan State University poultry farm on Jolly Road. This combination was selected after tests of several sands and sand-loam mixes in small chamber infiltration experiments because it exhibits a rate of infiltration which can be easily followed and because it does not shrink and crack while drying after an infiltration run. A gradation curve for this soil is shown in Figure 9. The specific gravity of soil solids for this experimental soil was 2.631.

Transmission Coefficients

Diffusivity function

The theory for two methods of determining the diffusivity function was developed in Chapter III. One method involves moisture content measurement during infiltration in a horizontal column at a fixed time, and the other requires measurement at a fixed position as time varies. A discussion of the experimental procedure used and results obtained follows.

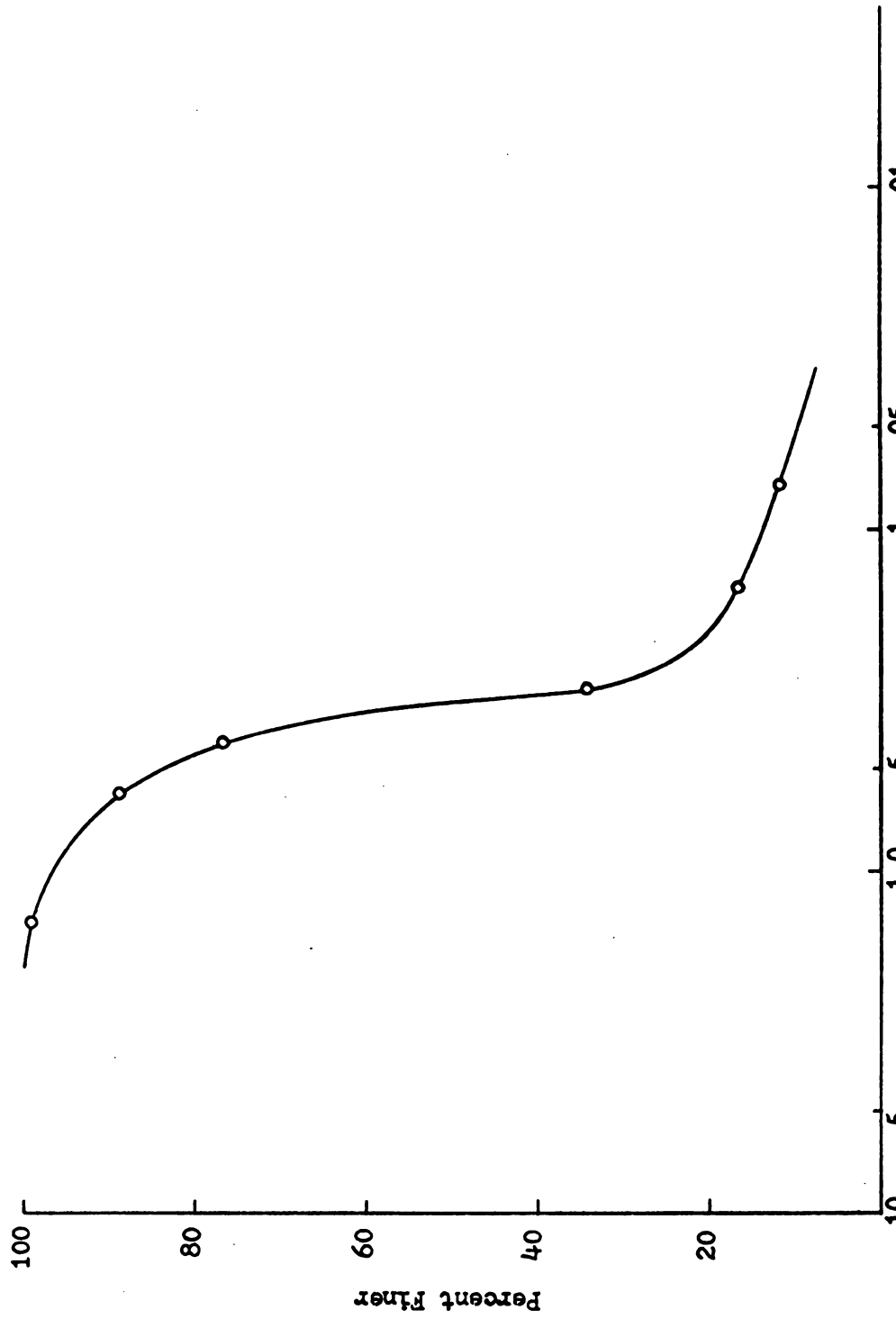

Figure 9. Gradation Curve From Sieve Analysis of Experimental Soil Mix

First, a sectionable cylindrical column was formed by cutting and machining 1-cm. rings from acrylic tubing with a 1 3/4-in. (4.43 cm.) inside diameter and 1/8-in. (0.312 cm.) wall thickness. Twenty 1-cm. rings were clamped together to form a column similar to that used by Bruce and Klute (1956). A 1/32-in. hole drilled in every other ring provided for air escape. The column was closed at one end and placed vertically for packing. An additional 6-cm. section of tubing was clamped to the top end to allow soil packing beyond the end of the test cylinder. Layers of soil 2 cm. thick were placed in the column and each tamped to duplicate the density of the soil in the large chamber. After the column, including the 6-cm. section, was completely filled and tamped, it was scanned with the gamma ray system described in Chapter IV to determine the density distribution along the length of the column. If the standard deviation in density exceeded .03, it was discarded and a new column packed until a column of uniform density between 1.68 and 1.70 gm/cc was achieved.

A headstock was formed to provide a water source at one end of the column from a 4-cm. length of tubing which was closed at one end and had a porous stone fitted in the other end. An air vent and elevated reservoir similar to that described by Bruce and Klute (1956) were provided for rapid filling of the headstock. A Marriotte flask supplied water at constant head, maintaining atmospheric pressure at the center of the horizontal column. Before an experimental run, the porous stone

was presoaked, and free water was removed from it just before it was clamped against the soil column. The headstock was then rapidly filled, requiring about three seconds, and infiltration began.

The diffusivity function was determined by both methods on the same column. The column was placed on a horizontal shelf attached to a movable frame so that the column could be positioned as desired in the gamma ray beam. Thus, moisture content variation at a fixed point could be determined with respect to time. As the advancing wetting front approached the section where gamma absorption measurements were made, consecutive 30-second counts were taken starting when the visible front was 2 cm. from the gamma beam and continuing until it was well past the beam and the count had stabilized. Following this procedure, it was possible to use the gamma beam at two positions along the column during a single infiltration.

The 30-second counts were plotted against time and a smooth curve drawn through the points to eliminate scatter due to the random emission of gamma radiation. Coordinates of count rate and time were then selected from the curve and a computer program written to solve first for the moisture content corresponding to the count at each time and then to solve a finite difference representation of equation 21. The equation used was

$$D(\theta_j) = \frac{1}{4} \frac{x^2}{t_j^{3/2}} \left(\frac{t_{j+1} - t_j}{\theta_{j+1} - \theta_j}\right) \sum_{i=1}^{j} \left[\left(\frac{1}{\sqrt{t_j}} + \frac{1}{\sqrt{t_{j+1}}}\right) \frac{\theta_{j+1} - \theta_j}{2}\right]_i \quad (43)$$

where x is the distance from the source to the point where measurements were taken; $D(\theta_j)$ is the diffusivity at moisture content, θ_j; and t_j is the time at which θ_j occurred in the infiltration column at the point x cm. from the source. A sample curve of counts versus time and data used in the computer program are included in the Appendix.

For the Bruce and Klute method, the moisture content distribution along the column at a fixed time is required. The flow was shut off and the headstock rapidly disconnected when the advance had traveled about 18 cm. The column was then quickly sectioned into 1-cm. sections and the moisture content of each determined gravimetrically. The sectioning process required about three minutes. Each section was placed into a soil tin and covered as it was sliced from the column.

A distance versus moisture content curve was drawn from the data resulting from sectioning the column. From this curve the slope $(\frac{dx}{d\theta})_{\theta_x}$ was evaluated and the integral in equation 20 was computed numerically. A computer program was written to carry out the solution of equation 20 for $D(\theta)$. A sample distance/moisture-content curve is included in the Appendix.

Five diffusivity curves were determined, three with the fixed position method and two with the fixed time method. These are shown in Figure 10 without data points for clarity. A curve complete with data points is included in the Appendix. To determine values of $D(\theta)$ for use in computer solutions, a curve formed by graphically averaging the curves in Figure 10 was used. It is plotted in Figure 11.

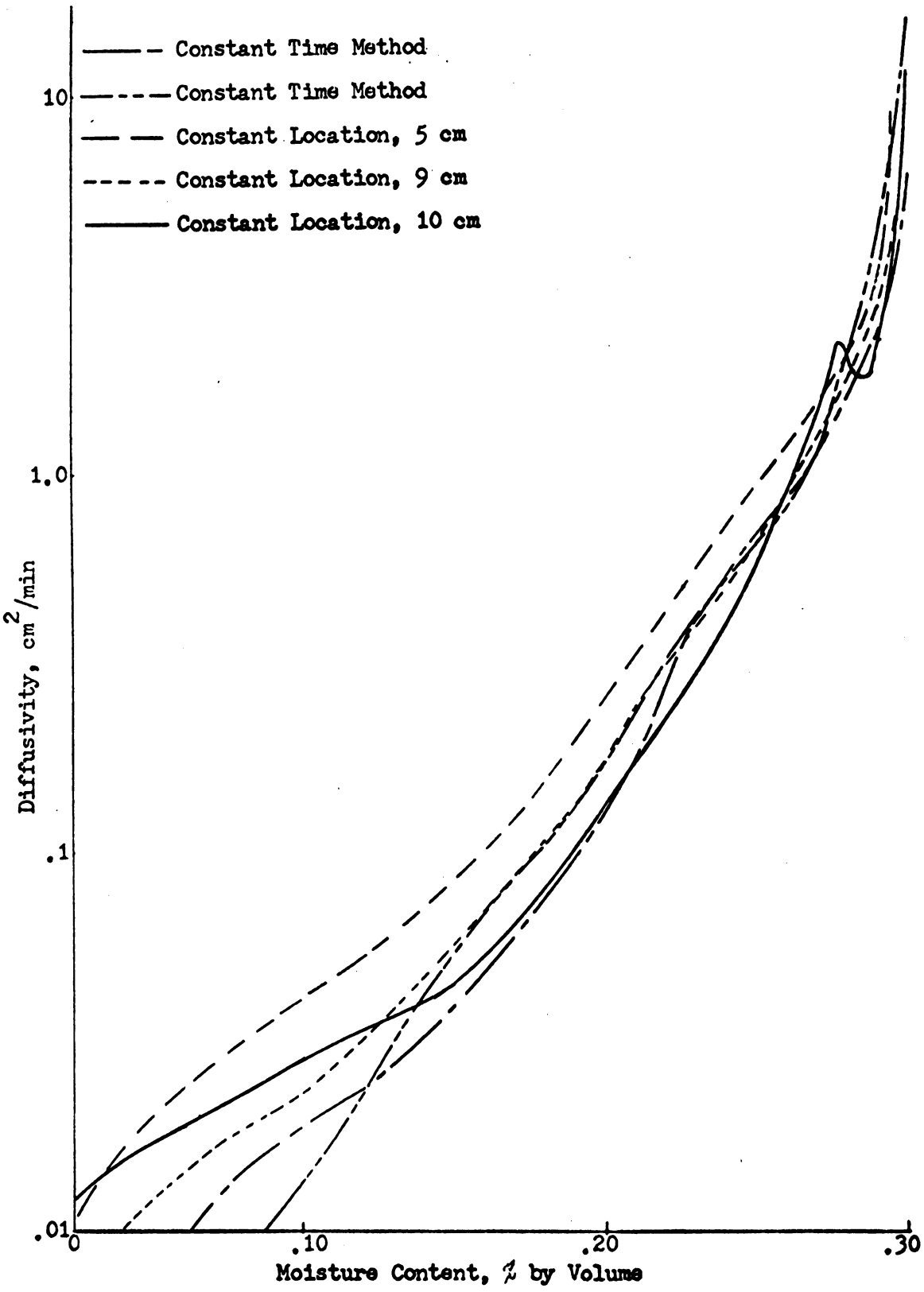

Figure 10. Diffusivity Curves for Experimental Soil Determined by Two Wetting Front Advance Methods

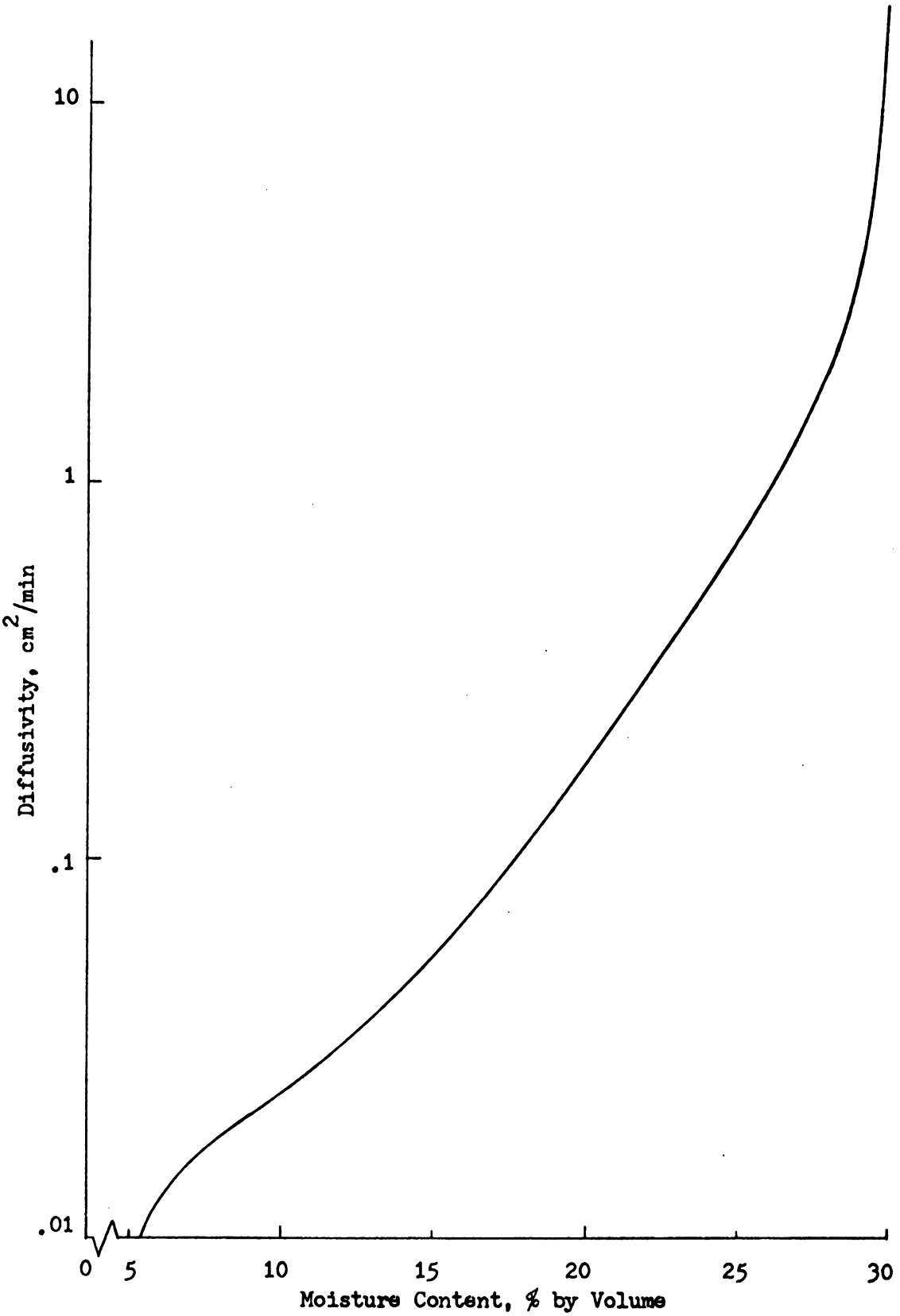

Figure 11. Average Diffusivity Curve for Experimental Soil Mix

Moisture-content vs. head relation

The moisture-content vs. head relation for the experimental soil was determined for both wetting and drying conditions. Soil samples were placed in small pressure cells[1] similar to those described by Klute (1965). For replication 10 cells were started, but one was accidentally dropped and had to be deleted from the test. Each cell contained a brass sample retainer ring 5.4 cm. in diameter and 3 cm. high which sat on a porous ceramic plate with a bubbling pressure in excess of 1 atmosphere. Pressure was supplied to each cell and an outflow tube was provided underneath the ceramic plate. The outlfow tube was placed in a tray of water and the water level kept within 1 cm. of the bottom of the porous plate. Provision was made so that the pressure supply line could be clamped off and disconnected for weighing the entire cell to determine moisture content change within the sample. These cells were well suited to determining an absorption curve, since the entire cell could be weighed and the moisture content of the sample determined without disturbing the contact between the sample and the porous plate.

To achieve 10 uniform soil samples, all 10 sample rings were removed from their cells and taped together in a continuous column. An extra 6-cm. length of tubing was added to the column, and the entire column was filled and tamped to achieve the desired density of 1.68 to

---

[1]Tempe Pressure Cells, Soil Moisture Equipment Co., Cat. No. 1400, Santa Barbara, Calif.

1.70 gm/cc using procedures similar to those described for the columns used in the diffusivity determination. After the column of rings was packed, it was scanned with the gamma ray equipment to determine the density variation along the column. The mean density and its standard error were 1.689 ± .0064. The column was moistened so that it could be sectioned with a wire soil saw without disturbing the ends of each sample. Rings were placed on presoaked porous plates. One wetting and drying cycle was performed before data were taken. For this preliminary cycle, the cells were placed in the tray and left until the samples ceased to take on weight. A pressure of 10 psi was applied and the cells were allowed to equilibrate. The pressure was then released, and after all cells had ceased to absorb water, the procedure was started to determine the wetting and drying moisture-content vs. head relationship for the soil.

Pressure increments of about 15 cm. H_2O were used in the initial stages of the desorption curve and the pressure step increased gradually to 100 cm. as the samples ceased to exhibit much change in moisture content with change in head. When the desorption curve had reached a nearly constant slope, at approximately 700 cm. H_2O, the absorption part of the cycle was started. As with desorption, at the higher head levels, larger pressure increments were taken and the size of the pressure increment decreased as the amount of absorption with each pressure increment increased. At each pressure step, the system was allowed to equilibrate until the average weight change of the cells was less than

0.1 gm. in 24 hours. The moisture-content vs. head relation is shown in Figure 12. Note that the absorption curve crosses the desorption curve in Figure 12 as saturation is approached. This is probably due to not allowing enough time for complete equilibration prior to starting the desorption cycle. Since subsurface irrigation is an imbibition or absorption process, the wetting curve is the one of interest for this study.

Conductivity function

To obtain the absorption water capacity function, the slope of the curve in Figure 12 was evaluated numerically. The water capacity function was evaluated for moisture content values corresponding to those used to evaluate the diffusivity function, and the conductivity was then calculated from the relation

$$K = DC \quad . \tag{44}$$

The resulting conductivity function is shown in Figure 13.

In addition to determining the unsaturated conductivity function, the saturated hydraulic conductivity was determined using a constant head apparatus. Sample rings 3 in. in diameter and 3 in. high were packed to a density between 1.68 and 1.70 gm/cc, placed in sample holders, and saturated overnight. A constant head of 3.8 in. was maintained between ponded water on the surface of the sample and the outflow tube below it. The conductivity after 12 hours of flow was

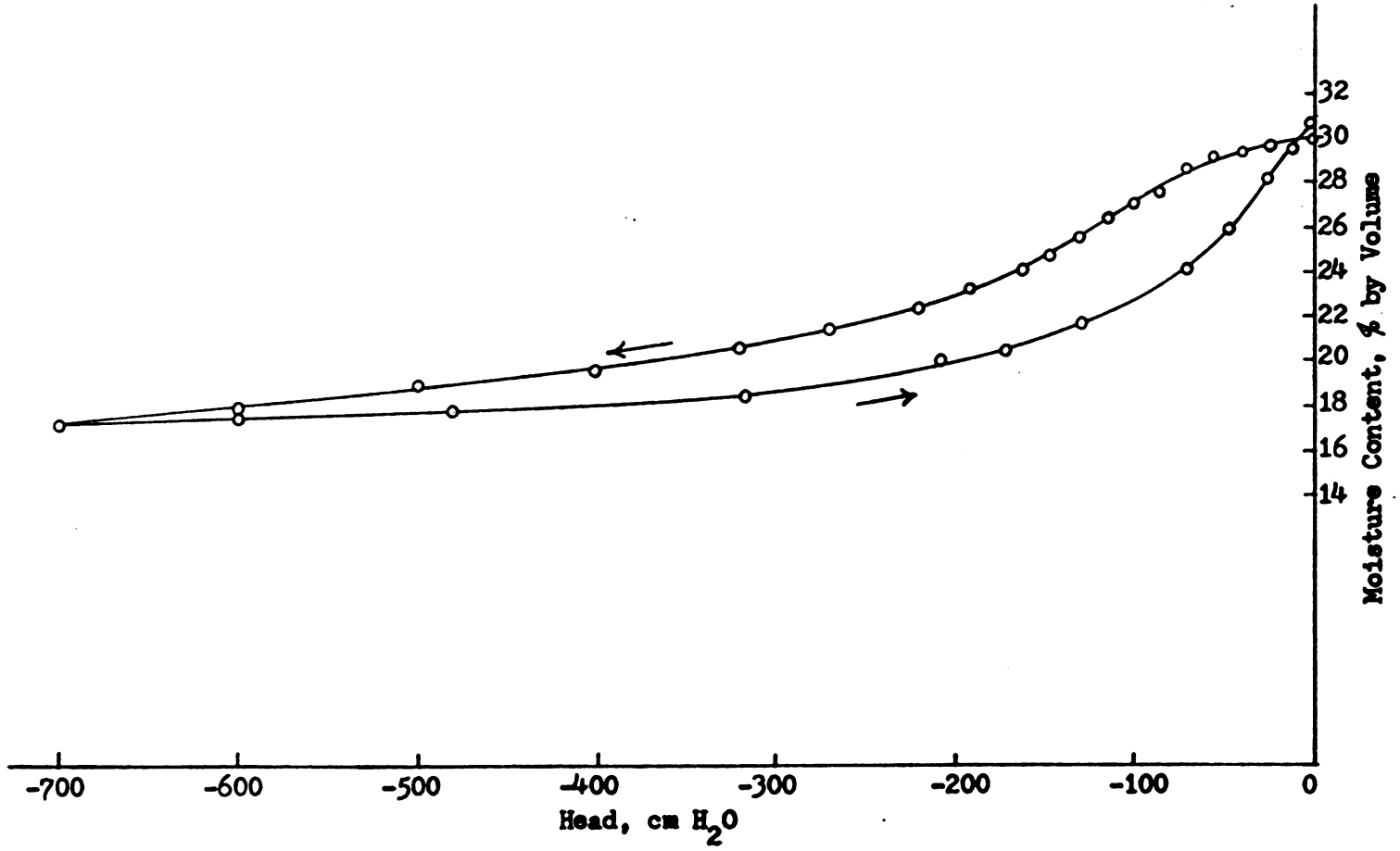

Figure 12. Moisture Content vs. Head Relation

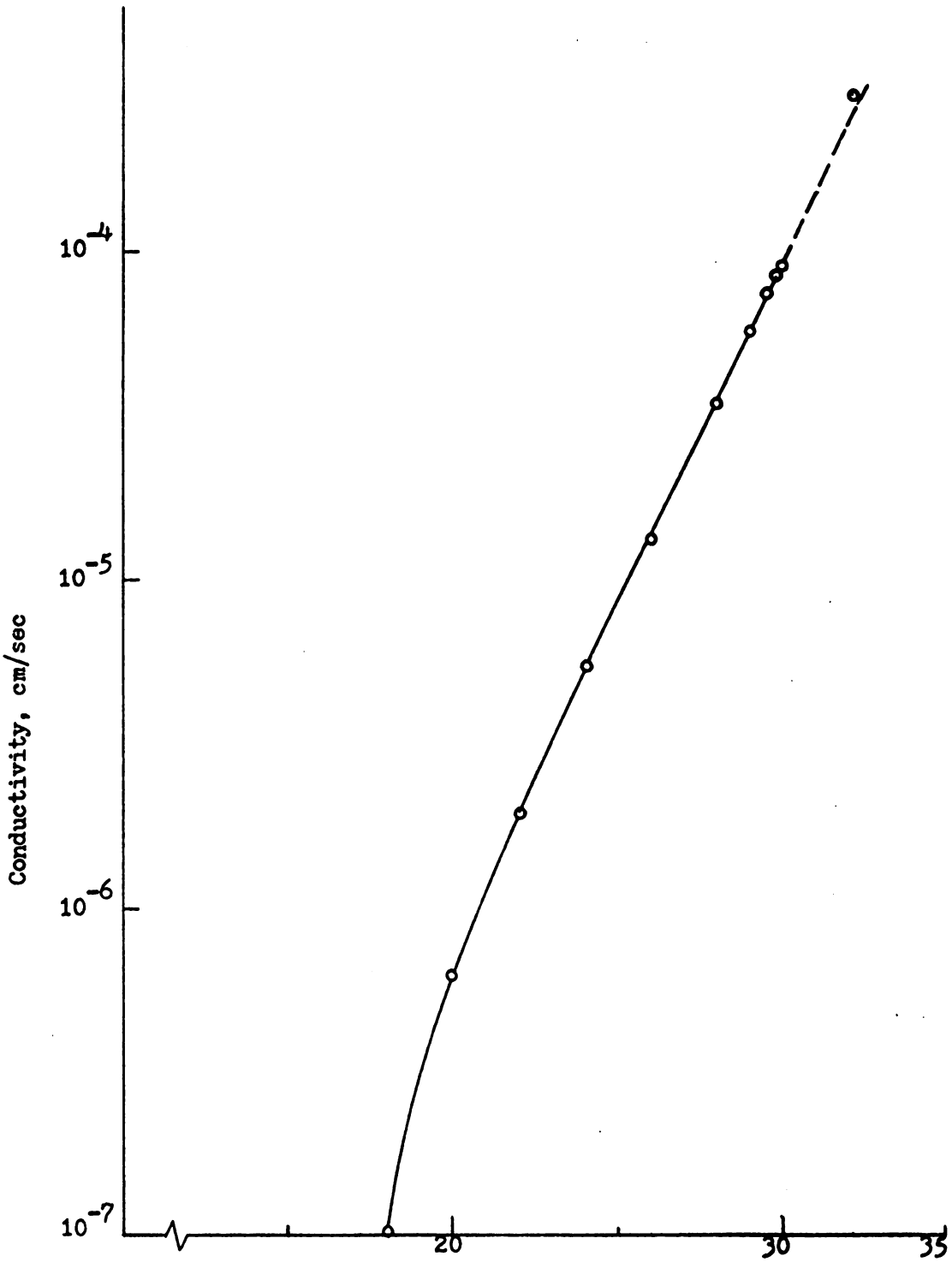

Figure 13. Unsaturated Conductivity Function
(Uppermost point is saturated conductivity)

measured, and the mean saturated conductivity from six samples was 3.067×10^{-4} cm/sec. The moisture content of the saturated conductivity samples averaged 32.2 percent. In figure 13 the uppermost point shown represents the saturated conductivity, and it is very close to being on an extension of the unsaturated conductivity curve.

VI. RESULTS AND DISCUSSION

Mathematical models of a complicated process such as infiltration from a buried moisture source cannot be used with confidence unless they are checked with results obtained by other means. One means of checking models and theory is the use of data obtained experimentally in a laboratory. In this study a soil chamber was used to study the infiltration process. Experimental results are compared with a simplified model to determine whether a simple one-dimensional model can be used to predict the wetted region around a buried moisture source.

Porous Pipe Characteristics

A knowledge of the flow characteristics of the porous plastic pipe used in the soil chamber is important because the flow from the pipe establishes the boundary condition at the source. This boundary condition must be used in simulating flow with a mathematical model.

Preliminary tests showed that flow through the porous ABS plastic pipe[1] used in this study would nearly cease after several days of continuous flow using unfiltered distilled water. Examining under a

---

[1]Trade name Micro-Por marketed by International Plastics, Inc. 9/16" (14mm) OD, 7/16" (11 mm) ID.

microscope thinly sliced cross-sections from a pipe which had ceased to flow did not reveal the cause of plugging. Figure 14 shows how flow rate of unfiltered distilled water through a new 1-ft. section of the porous pipe decreased with time. After water had flowed through the pipe for nearly 30 hours, the pressure in the pipe was increased, resulting in an increase in the flow rate, which then dropped off relatively rapidly. Fine filtration was required to maintain flow at a constant rate. In all subsequent tests with the porous pipe, a 0.45 micron millipore filter was used to filter distilled water containing 0.1 percent phenol before it reached the pipe.

Discharge through the walls of the porous pipe varied with internal pressure. To test the magnitude of this variation, ten 1-ft. sections of pipe were connected simultaneously to a variable head reservoir. Pressure was measured at the plugged end of one lateral and flow rate was determined by weighing the outflow, which dripped from the horizontal pipe sections and was caught during a measured time period chosen to produce approximately 500 gm. of outflow. Figure 15 shows the average-discharge vs. head relation found for the ten sections of pipe using distilled water.

The range of discharges at a fixed pressure was great for these ten samples. It is not known whether the 1-ft. samples were cut from the same or different lengths of pipe because they were supplied by the company as individual samples.

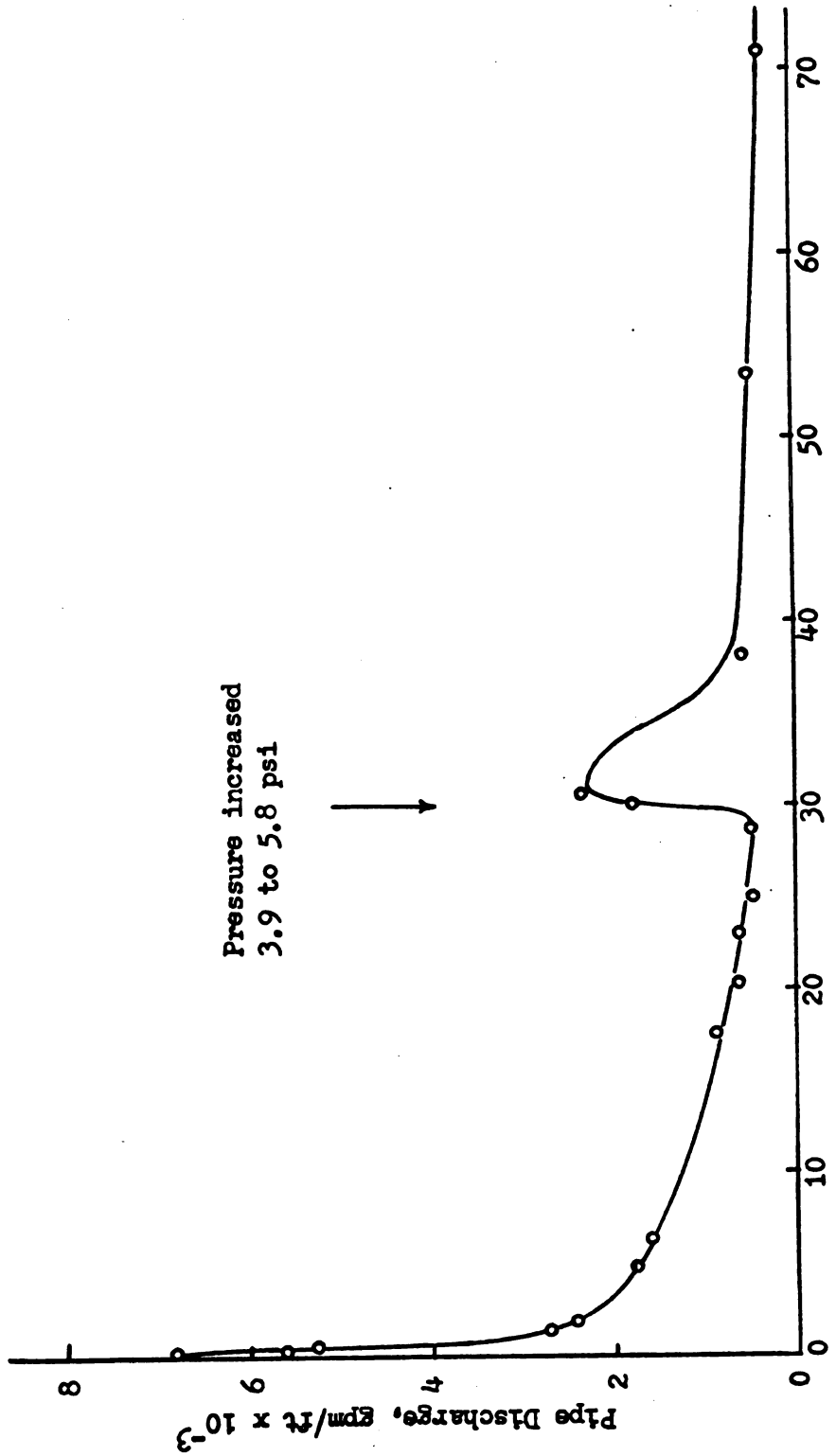

Figure 14. Porous Pipe Discharge to Air Using Unfiltered Distilled Water

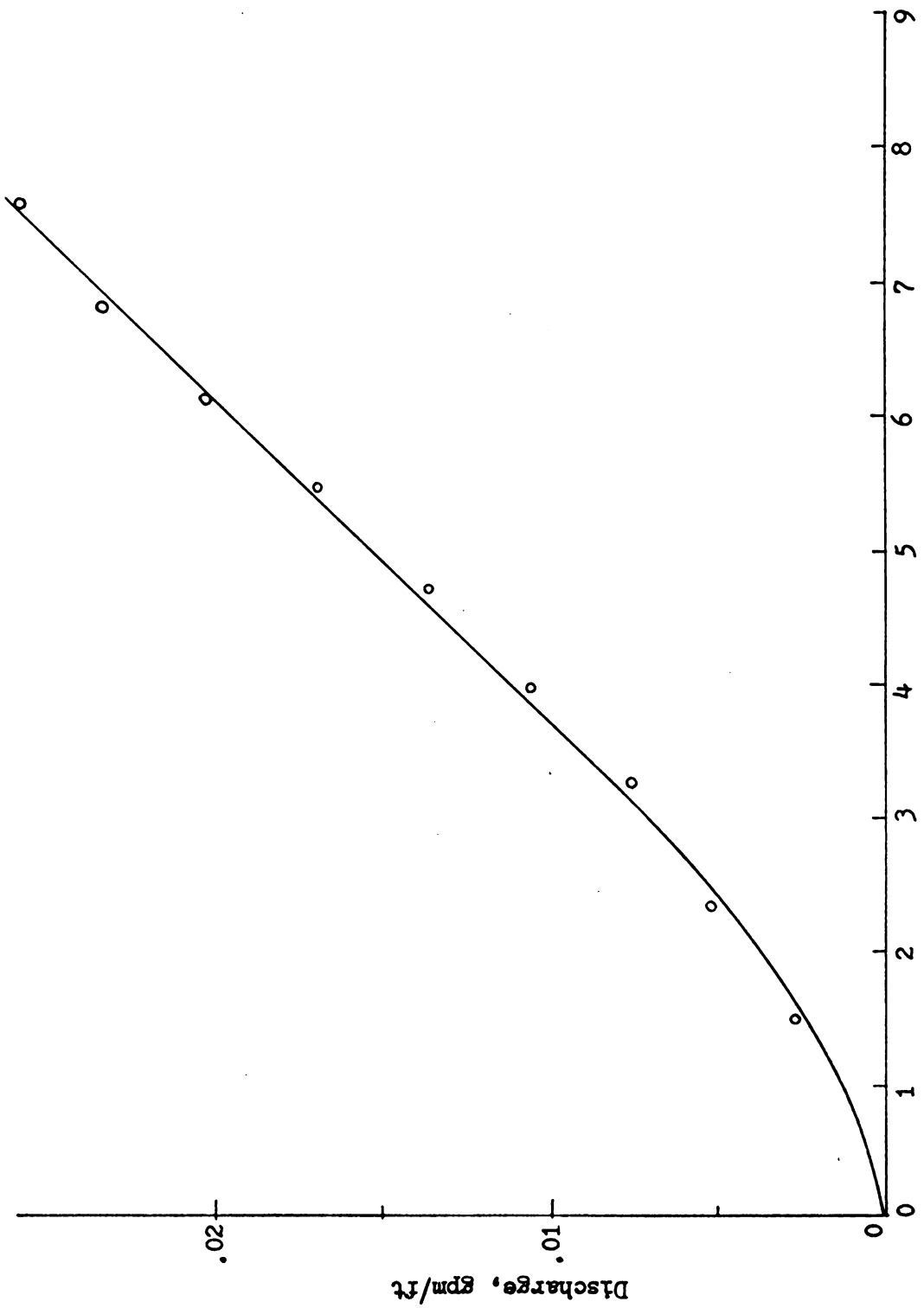

Figure 15. Average Discharge vs. Head Relation for Ten 1-Ft. Sections of Porous Pipe

For internal pipe pressure between 3 and 7 ft. of water, the outflow-head relation was approximately linear. The slope of the curve in the linear region was 0.0042 gpm/ft. per ft. of head with a standard error of ± 0.00092.

The discharge rates were approximately twenty times the average discharge found by Wilke (1970) for 100- and 470-ft. Micro-Por^{tm} laterals buried in the soil. When a section of the pipe was installed in the experimental soil chamber, the discharge still exceeded that reported by Wilke by an order of magnitude. The difference could have been related to the filter used, as Wilke used a 5 micron cartridge filter, and a 0.45 micron membrane filter was used in these tests. Another source of difference is that Wilke measured pressure and flow rate at the lateral inlet so that he related maximum lateral pressure to average discharge along the lateral.

The section of porous pipe used in the soil chamber was cut from the 1-ft. section having flow characteristics closest to the average of the ten sections tested to obtain the curve shown in Figure 15. This 3 1/4-in. (8.23 cm.) section of pipe exhibited flow rates ranging from 7 to 12.5 ml/min. during infiltration tests with the soil chamber. This range of flow rate would be equivalent to an application of 12.1 to 20.6 cm/day from a subsurface irrigation system with laterals spaced 40 in. apart. A subsurface irrigation system with application rates of this magnitude would certainly be operated in an intermittent rather than a continuous manner. To design an intermittently operated system,

it is important to be able to predict the development of the wetted region around the source.

Initial and Boundary Conditions

Much of the literature concerning infiltration from a buried source assumes that water enters the soil around the source at or near atmospheric pressure. A constant flux boundary condition can also be used at the source, but for the conditions of this study, neither of these popular boundary conditions occurred exactly. Instead, a small saturated zone of positive pressure developed around the source. The flow rate from the source was not found to be constant, but part of the variation experienced was due to the lack of a precise control system for maintaining a constant pressure within the source. The saturated region enlarged until the circumference of the region was large enough that the rate of flow from the circumferential boundary of the saturated region under unsaturated flow conditions equaled the inflow from the source. After an initial rapid growth, the saturated region slowly grew to a maximum radius of 3 to 4 in.

The size of the saturated region was determined by inserting flexible capillary tubes 1/2 in. apart through the acrylic face of the soil chamber. They were placed along the horizontal axis on the opposite side of the source from that scanned by gamma ray and also just off the vertical axes. Static capillary rise in these tubes was approximately 0.5 cm. Figure 16 shows the positions of the capillary tubes

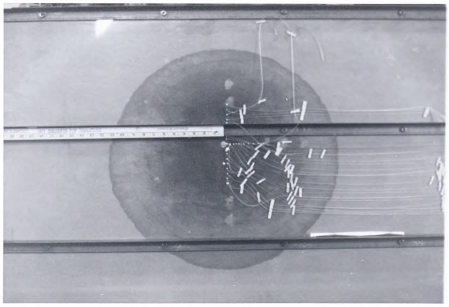

Figure 16. Positions of Capillary Tubes on Soil Chamber for Determining Positive Pressure During Infiltration Run

during an infiltration run. Additional tubes were inserted near the source, and when the pressure in the soil moisture at the inlet to a capillary became positive, water moved into the capillary. The saturated zone was considered to be the area where positive pressure was found. The relation between the radius of the unsaturated zone, r_0, and the time from initiating infiltration, t, is of the form

$$r_0 = a_0 + a_1 \ln t \quad . \tag{45}$$

The coefficients a_0 and a_1 were found using linear regression with ln t as the independent variable. Relations for the growth of the saturated region in the horizontal, vertically up, and vertically down directions are shown in Figure 17 for the initial condition of air dry soil.

During the experiments, the growth of the saturated region vertically up from the source seemed to exceed the growth vertically down. After running regression analyses, the slope of the r_0 vs. ln t relations were compared for the two vertical directions and found to be different at the 95 percent confidence level, indicating that the data support the laboratory observation of more rapid saturated region growth vertically upward. Data for other initial moisture contents showed the same result.

The initial condition for infiltration tests was a constant moisture content throughout the soil. While a spatially varied initial moisture content could be handled with the computer program, such an initial condition would have been difficult to establish with the

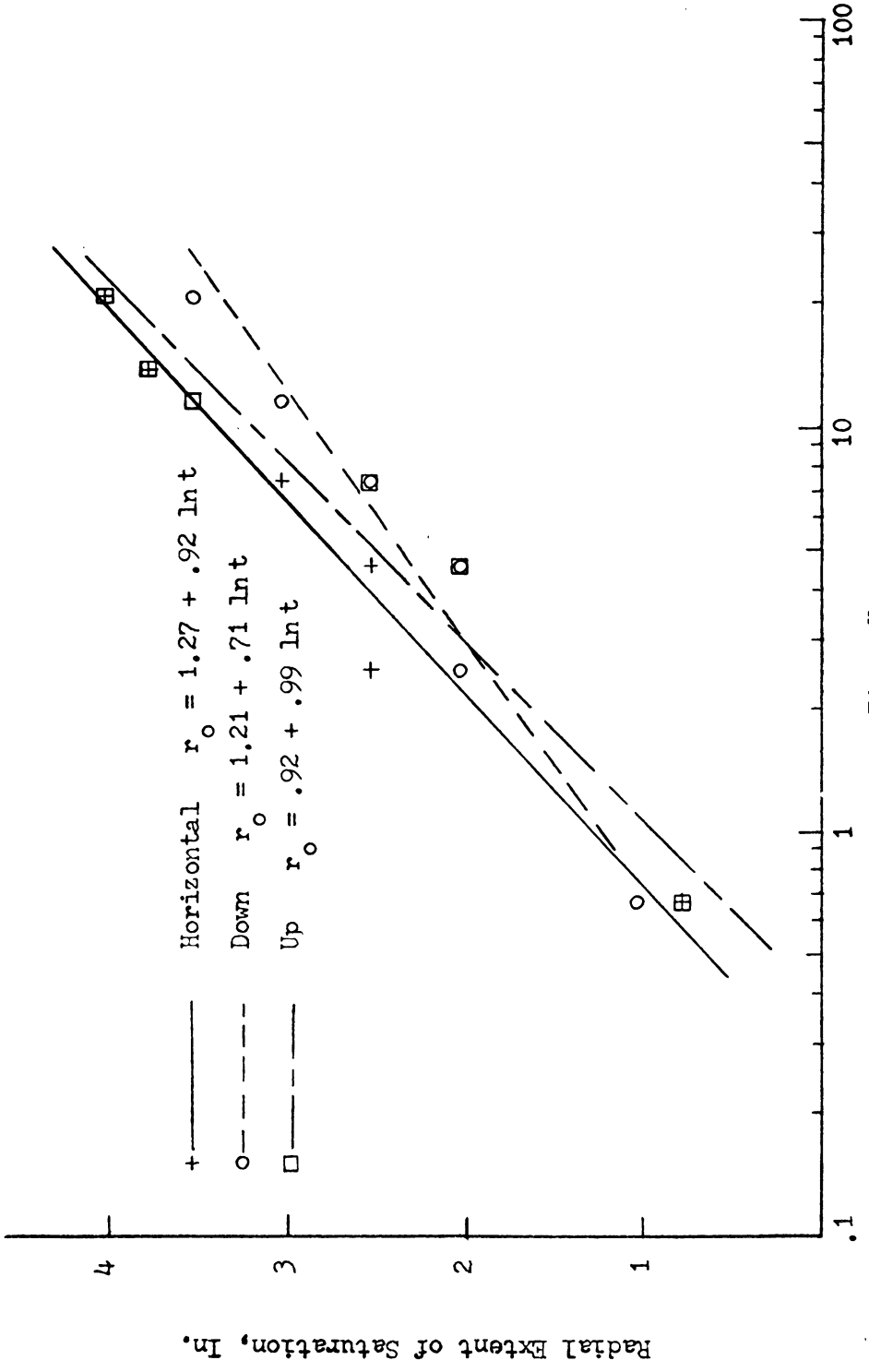

Figure 17. Distance from Source Center to Outside Edge of Saturated Region in Three Major Directions for the Air Dry Initial Moisture Content

experimental set-up used. Infiltration trials were conducted into air dry soil having a volumetric moisture content of about 1.8 percent and into soil at about 10 percent moisture content. Initial moisture contents greater than 12 to 14 percent could not be easily used because of the difficulty in following the advance of the wetting front visually. At higher moisture contents there was no perceptible color change at the wetting front. Following the wetting front with the gamma ray system was not possible because the system did not have a rate meter, and locating the wetting front by successive counting in fixed positions would have been a slow process.

The initial moisture content for an infiltration experiment was established by drying the soil after moisture had been allowed to redistribute following the previous run. Figure 18 shows a typical saturation distribution along the three scanned axes after redistribution. The moisture content was fairly uniform except for higher values near the bottom of the chamber and a decrease at the edge of the wetted region in the horizontal direction.

Although there was no exact control over the establishment of the initial moisture content conditions for a given test, by allowing the soil moisture to redistribute after infiltration and timing the drying period carefully, relatively uniform moisture contents in the desired range were achieved. Figure 19 shows the variation in initial moisture along the three major axes for a run with an initial moisture content averaging 11 percent.

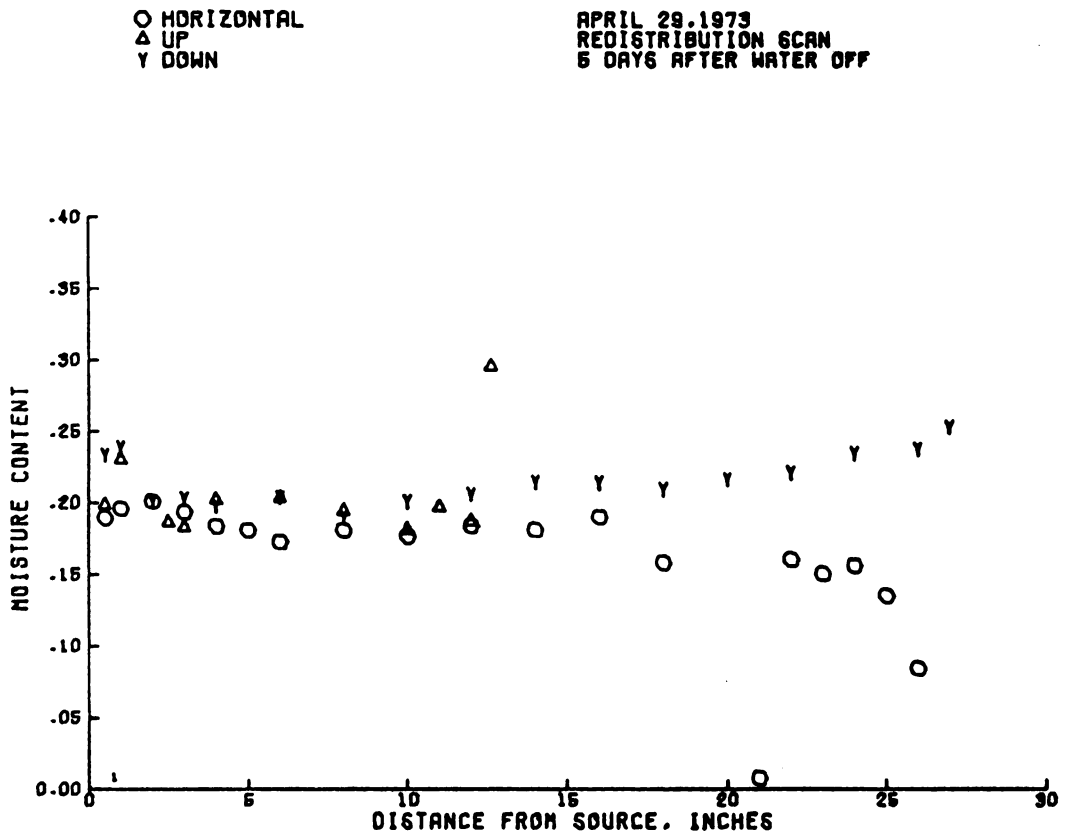

Figure 18. Moisture Content vs. Distance from Source in Three Major Directions Five Days After Infiltration

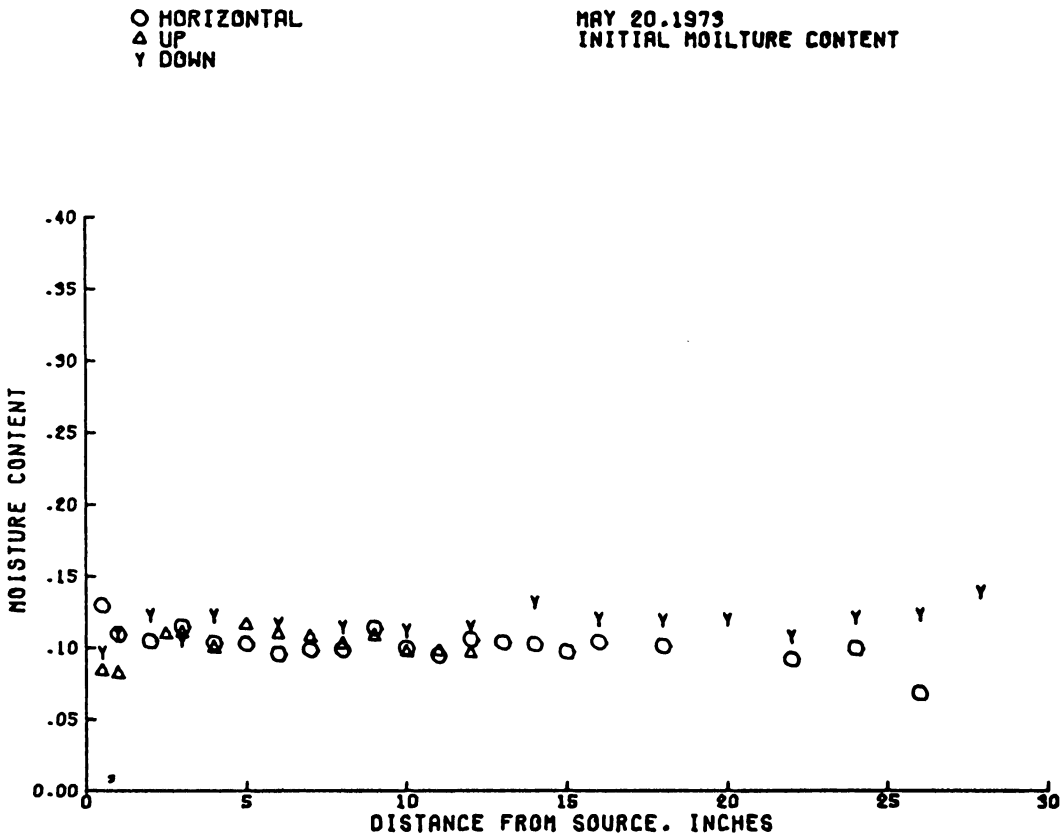

Figure 19. Initial Moisture Content Distribution in Three Major Directions from the Source

Use of Mathematical Model

The one-dimensional diffusion equation for radial flow and an appropriate numerical solution which were discussed in Chapter III were used to compute radial flow in each of the three major directions from the source to compare with experimental results. Experimental data on the growth of the saturated region around the source were used to establish the boundary condition at the source. Essentially, the source boundary condition was a moving boundary condition as the saturated region grew. The location of atmospheric pressure moved from near the source early in the infiltration process to a point 3 to 4 in. from the source near the completion of the test.

The solution for infiltration along one axis was essentially a two-step process. The first step involved the use of soil moisture transmission coefficients evaluated at a time when the saturation distribution was known to solve for the saturation distribution at one-half time interval forward. Results of computations for the half-time interval were then used in the second step to evaluate transmission coefficients for computing the saturation distribution at the end of the complete time interval.

In the solution of the equation, a constant grid spacing of 0.5 or 1.0 cm. was used in the r direction. The time increment, however, was varied--starting with small time increments near time zero when the saturation near the source was changing rapidly and then increasing the time increment to larger values as the wetting front moved farther from

the source. Computer runs using different time increment growth schemes were tried in order to determine appropriate time increments. The allowable increase in the time increment was chosen to avoid excessive deviation of the resulting solution from the solution using small time steps for the same condition. Time increments chosen for solutions ranged from 0.5 seconds for the first few seconds of infiltration to 250 seconds for times greater than 30,000 seconds.

To achieve a complete solution for a given set of flow conditions, the computer program was executed three times--once for the horizontal direction, once for vertically up, and once for vertically down. These three solutions gave the saturation distribution in each of the major directions and the wetting front position as a function of time.

Advance of the Wetting Front

The visual advance of the wetting front was determined every few minutes or few hours during the experimental process, depending upon the rate of advance. Figures 20, 21, and 22 show the advance of the wetting front in the three major directions plotted against time for initial moisture contents of 1.8 percent, 9.6 percent, and 11 percent, respectively. The points are experimental results, while the lines are calculated using the one-dimensional mathematical model. The v-shaped symbols used for advance up and down are oriented to point in the appropriate direction and plotted so that their points fall on the data points. Visual wetting front advance data were generally not collected

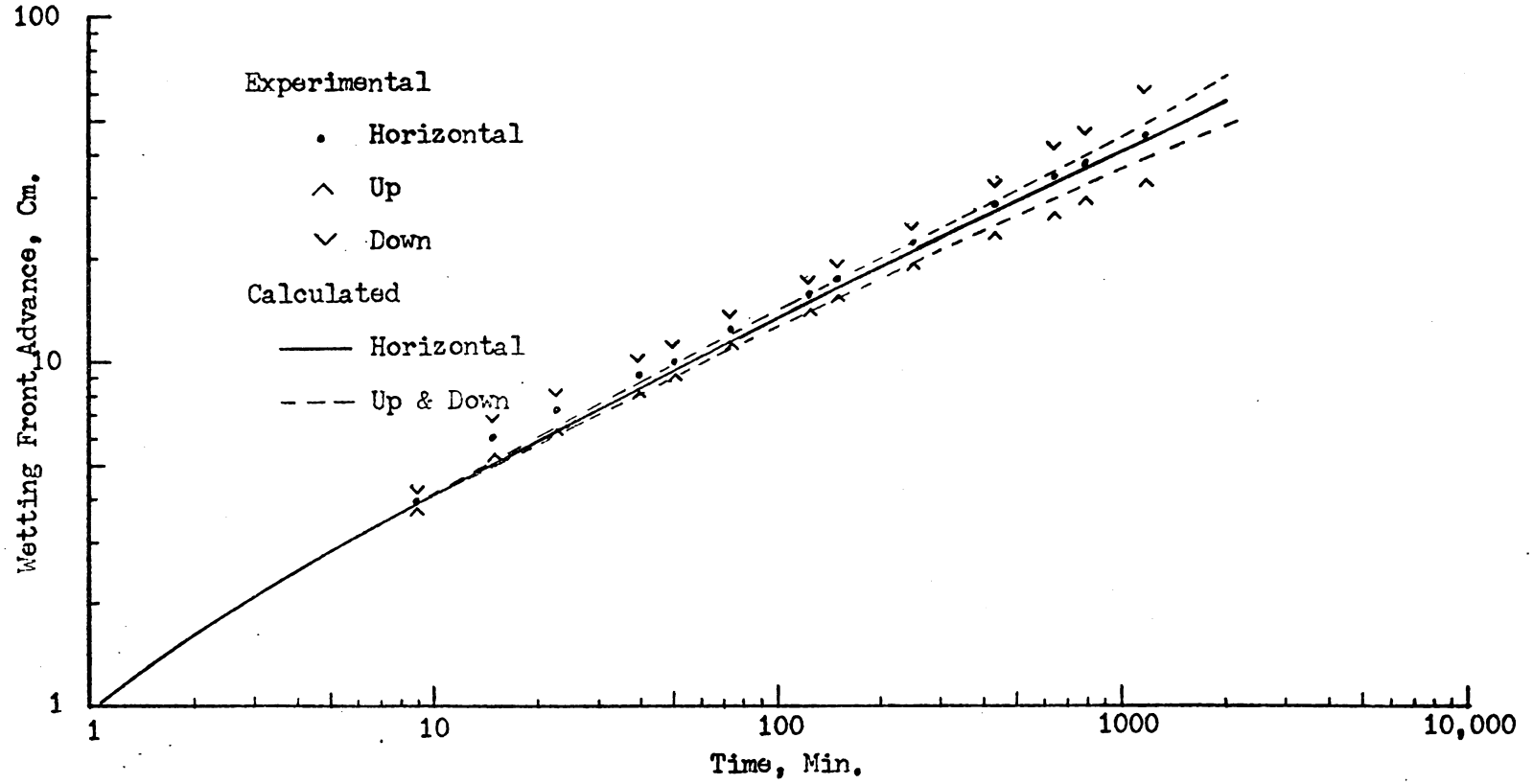

Figure 20. Experimental and Calculated Advance of the Wetting Front for an Air Dry Initial Moisture Content (θ_i = 1.8)

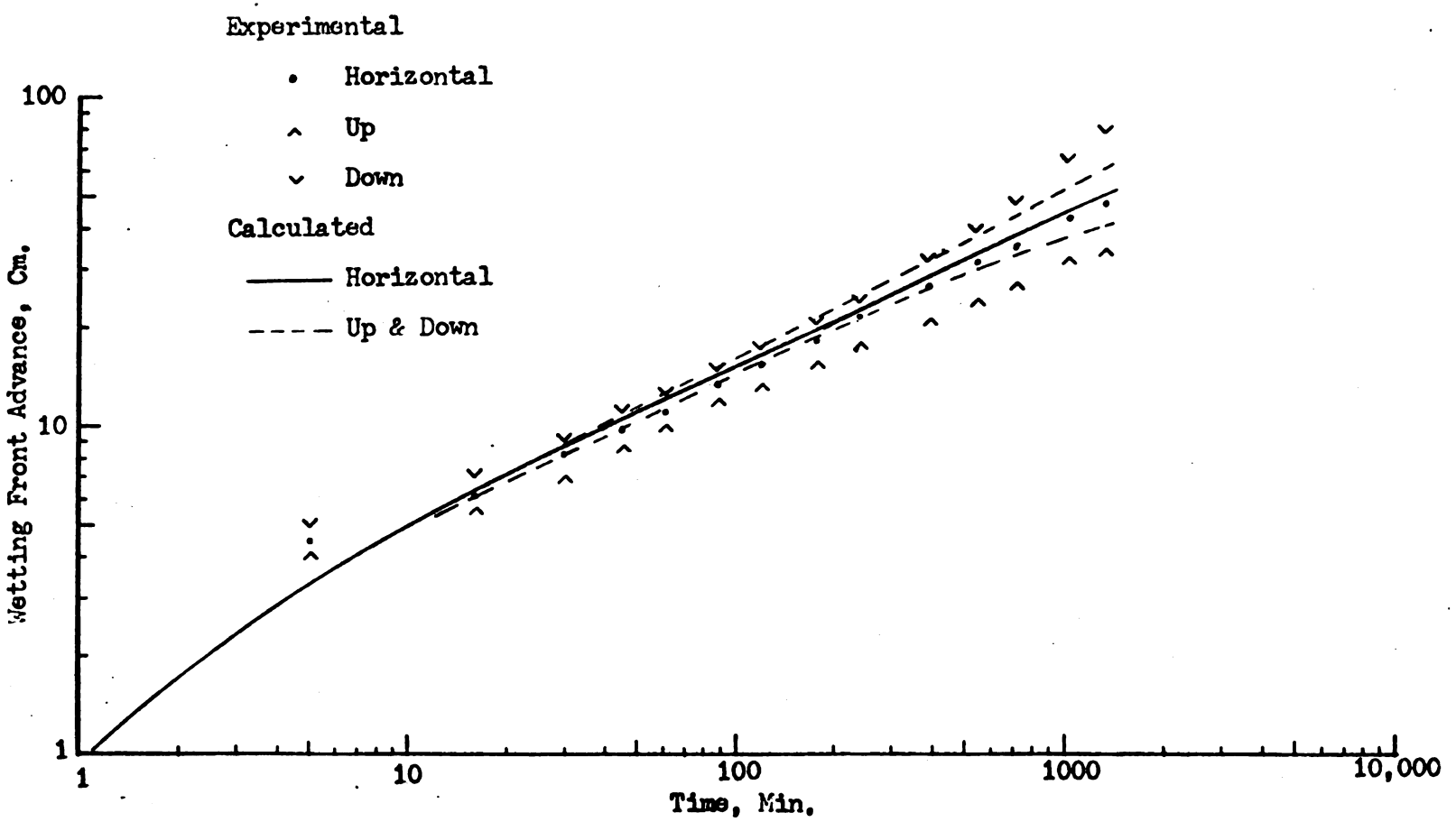

Figure 21. Experimental and Calculated Advance of the Wetting Front for an Initial Moisture Content of 9.6%

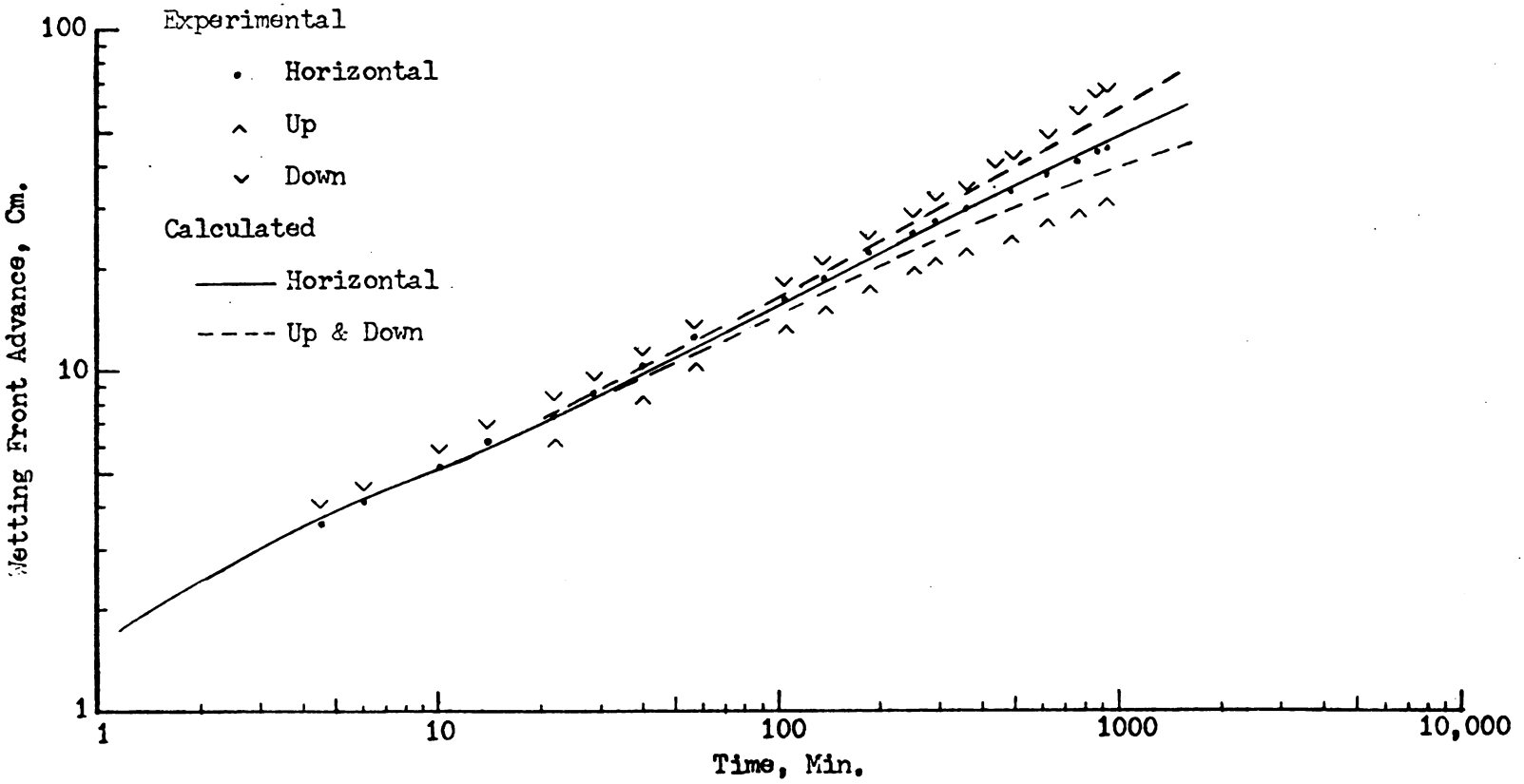

Figure 22. Experimental and Calculated Advance of the Wetting Front for an Initial Moisture Content of 11%

for times less than 10 minutes because this time was required to establish and stabilize pressure and flow. There is reasonable agreement between the experimental wetting front advance data and the calculated advance in the horizontal direction.

For the initially air dry soil shown in Figure 20, the experimentally determined horizontal advance was greater than the computed horizontal advance. This difference may have occurred because the one-dimensional model does not account for flow entering a horizontal wedge from the soil region above. While most of the water entering the upper boundary of the wedge would be expected to pass through and flow out the bottom boundary, it would still contribute to radial horizontal movement.

For the advance curve shown in Figure 21, the computed horizontal advance leads the experimental advance. This could be caused by lack of agreement between the growth of the saturated region used as a boundary condition around the source in the model and that which actually occurred experimentally. All data on the growth of the saturated region for experiments with average initial moisture contents between 9 and 11 percent were pooled to determine the source boundary condition used for computing infiltration in this range of initial conditions. Figure 22 shows good agreement between computed and experimental wetting front advance for an initial moisture content of 11 percent.

For the case of flow both vertically up and down from the source, the model does not adequately account for the effect of gravity on the flow. As suggested in the discussion of the one-dimensional model in Chapter III, the model accounts for the effect of gravity on the driving potential, but it does not account for the curvature of flow lines which occurred. Thus, the advance in the upward direction was less than predicted by the model and the advance in the downward direction was greater than predicted. To predict adequately the vertical advance of the wetting front, a complete two-dimensional model of the flow is required.

Figures 20, 21, and 22 show that advance in the horizontal direction, when plotted against time on a log-log scale, resulted in an approximately linear relation after the first few minutes of flow. However, the flow in both vertical directions diverged from a straight line as time increased. As indicated in Chapter I, Smith (1966), Whitney et al. (1966), and Bush and Kneebone (1966) have all published results on advance of the wetting front in the three major directions in the form

$$r = at^n \quad , \tag{1}$$

but the results from this study indicate that this relation is valid only for horizontal flow. Horizontal advance curves from experimental data are plotted in Figure 23 for initial moisture contents of 1.8 percent (air dry) and 11 percent to show the effect of initial moisture content on advance. The slopes of the linear sections of the two

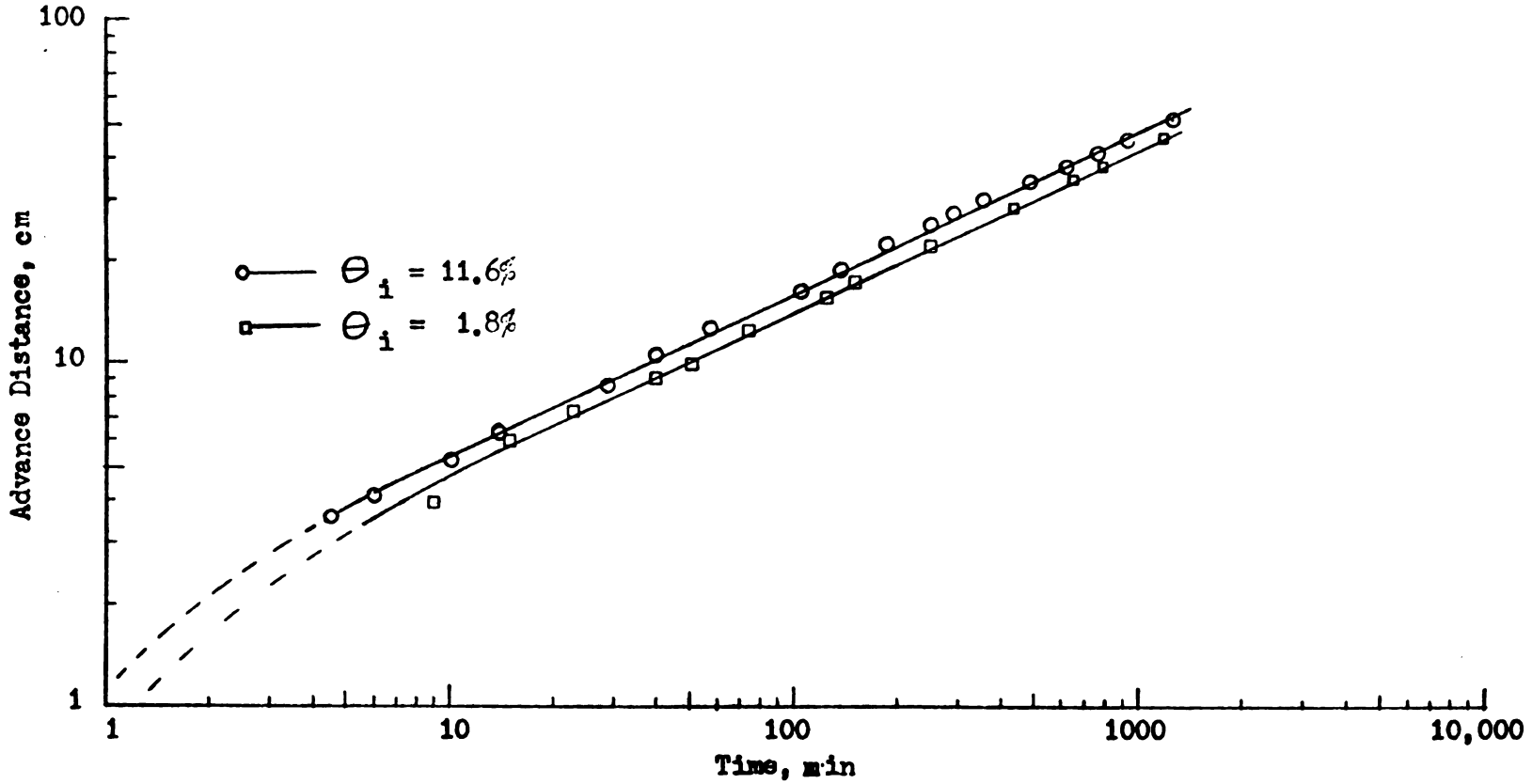

Figure 23. Horizontal Wetting Front Advance for Two Different Initial Moisture Contents

curves are similar, with the slope for the higher moisture content being 0.487 and that for the lower moisture content being 0.470. Slopes for other initial moisture contents were found to be very close to 0.47. Fitzsimmons (1972) reported slopes for horizontal advance in radially symmetric flow into a horizontal wedge and also found the slope of the linear portion of the curves to be approximately 0.47. The slopes determined here and Fitzsimmons's slopes are comparable even though he plotted time in seconds, since the slope of a log-log plot is dimensionless.

During each infiltration experiment, the wetting front location was traced on the acrylic face of the chamber at various times. Figure 24 shows the position of the wetting front at various times during infiltration for initial moisture contents of 1.8 and 11 percent. These tracings of the wetting front positions show that during early flow times the flow was nearly symmetric about the source. A slight gravitational effect appeared early in the flow and then the pattern advanced symmetrically for a time. This is indicated by the fact that in Figure 24 the wetting front position at one-half hour was somewhat farther below the source than above it, but the distance between the wetting front locations for the next two time intervals was not appreciably different above the source than below it.

As the wetting front advanced farther from the source, the effect of initial moisture content can be seen in the rate of wetting front advance downward. Comparing the 8- and 12-hour curves for the two runs

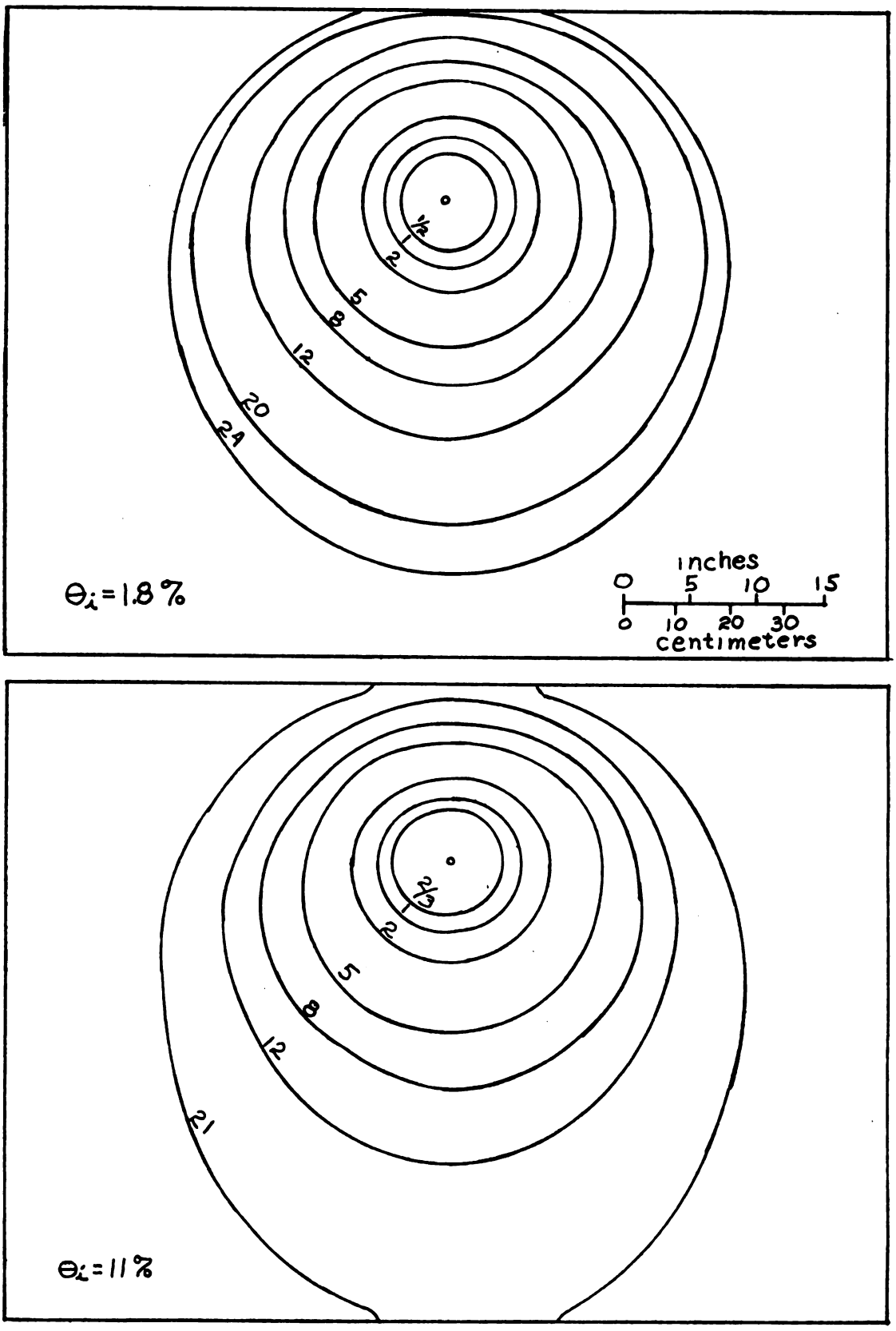

Figure 24. Wetting Front Position at Various Times During Infiltration (Numbers indicate time since beginning in hours)

shown in Figure 24 or the 12- and 20-hour curves at the top of Figure 24 with the 12- and 21-hour curves at the bottom, the effect of initial moisture content on the advance of the wetting front is obvious. The rapid advance shown by the 21-hour curve in the bottom few inches of the chamber for the 11 percent initial moisture content may be due to a slightly higher initial moisture content there.

It should be noted that while the analysis herein described has considered the movement of the wetting front along a horizontal axis through the source, the maximum lateral movement of the wetting front occurred below the level of the source. The maximum difference between the wetting front advance along the axis through the source and the maximum lateral advance was generally 2 to 3 cm. Therefore, a design based on the mathematical model proposed could result in subsurface irrigation laterals placed slightly closer together than necessary. However, if the advance along a horizontal axis through the source can be predicted with reasonable accuracy, that should be acceptable for spacing design purposes considering the uncertainty of the transmission coefficients and other variables, especially since the designed spacing would be conservative.

Moisture Content Distribution

Several times during each infiltration the chamber was scanned in each of the major directions to determine the moisture content distribution along the axes. Counts of 30 seconds' duration were taken every

inch with the gamma ray moisture sensing system. The moisture content distribution along each of the three axes after approximately 14.5 hours of infiltration is shown in Figure 25 for an initial moisture content of 11 percent. The computer-plotted points show percent saturation calculated from gamma ray counts along each of the three axes, and the broken line is the saturation distribution computed from the one-dimensional model for horizontal flow. The experimental data showed rather wide variation from point to point. The computer was programmed to compute saturation rather than moisture content from gamma ray counts to eliminate some of the variation. In computing saturation at each point, the soil density at each point is used so that variation caused by soil density nonuniformity is eliminated. Some of the variation could have been eliminated by taking longer counts, but longer counts were not taken in the interest of scanning all three axes as rapidly as possible to determine the moisture content distribution in all direction at about the same time.

The percent saturation as calculated from gamma ray measurement at various points in the chamber never indicated complete saturation, even near the source. In general, maximum saturation values were in the range of 0.85 to 0.9. This may have been due to air entrapment in the soil which prevented saturation from reaching 100 percent or could have been partially due to errors in measurement. Errors in the determination of the mass absorption coefficient for water or the specific gravity of soil solids could result in errors in the computed

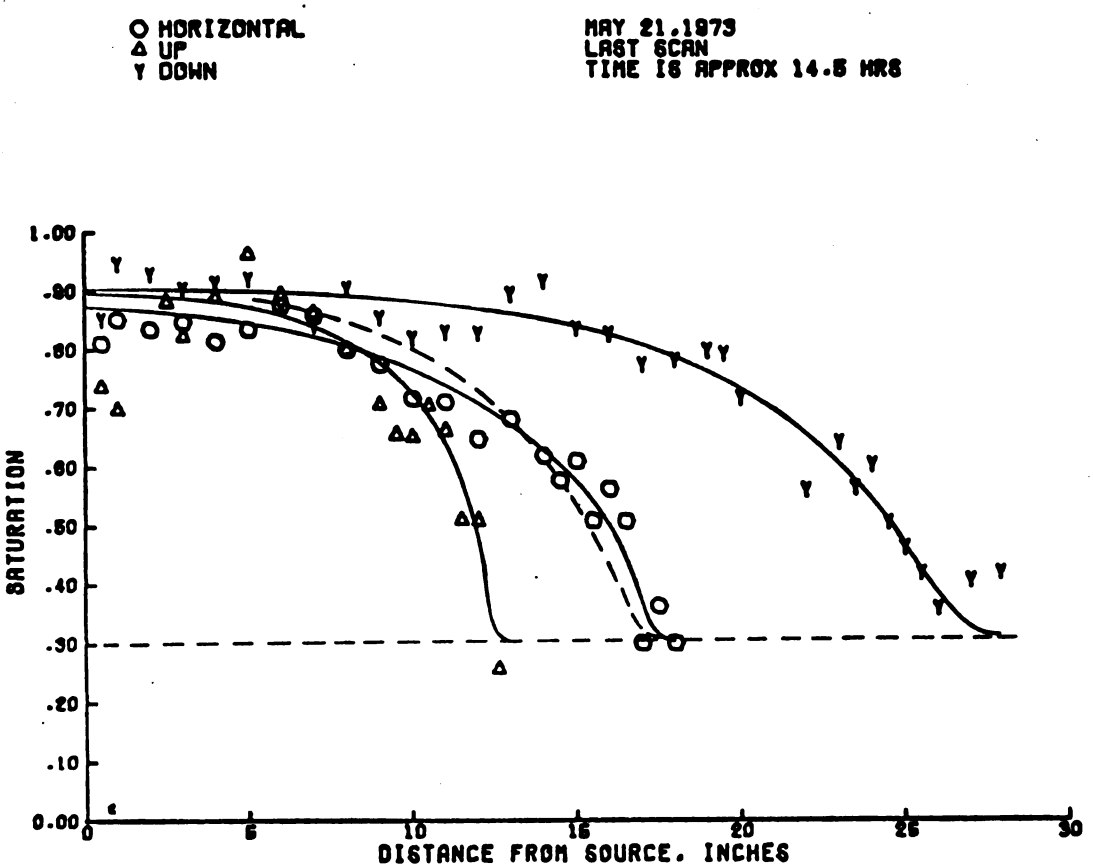

Figure 25. Saturation Distribution along the Three Major Axes 14.5 Hours after Starting Infiltration into Soil Initially at 11% Moisture (30.8% Saturation)

saturation. However, the size of the errors required to change the computed saturation from the values obtained to 100 percent makes it inconceivable that the deviation would be due to errors alone.

The saturation distribution during infiltration was obtained primarily for comparing results from the experiment and the mathematical model. The broken-line curve in Figure 25 was computed assuming a source boundary condition of 90 percent saturation. Considering the variability in the experimental saturation distribution data, the computed horizontal distribution is in reasonable agreement with the experimental results.

Implications

This study indicates that the horizontal advance of the wetting front can be approximated by a one-dimensional solution of the diffusion equation. While redistribution of the water after infiltration was not carefully studied, it was observed that during the redistribution phase, water movement was primarily vertically down. For the case of subsurface irrigation where the water is shut off when the horizontal advance from adjacent laterals comes close to meeting, redistribution will be characterized almost entirely by downward movement. Therefore, even an accurate prediction of the downward advance during the time the water is on would not accurately describe the final depth of infiltration.

It is anticipated that in some situations, considerations such as the depth of the homogeneous soil layer, plowing depth, and equipment available for installation of subsurface laterals may influence the depth of placement. Consequently, there may be times when the depth is more or less fixed and a design is needed for the spacing. If for an intermittently operated system it is known that a fixed quantity of water is to be applied during each irrigation, then the spacing can be determined by the distance the lateral wetting front would move in the time required to apply the desired amount of water. In such cases it may be possible to design lateral spacing based on a one-dimensional solution such as investigated in this study if representative soil moisture transmission coefficients can be determined.

VII. SUMMARY AND CONCLUSIONS

Moisture movement from a subsurface irrigation source was simulated in a large soil chamber with water entering soil at an initially uniform moisture content. Measurements were taken on the advance of the wetting front as a function of time, the rate of inflow from the source into the soil, the location of the saturated region around the source, and the moisture content distribution along horizontal and vertical axes through the source.

The differential equation describing one-dimensional radial flow was solved numerically using a predictor-corrector method for conditions along each of the three major directions from the source. Results were compared with experimental results to determine whether the one-dimensional model could be used to predict the advance of the wetting front from a subsurface source.

For the silty sand soil used in the test, the saturated region around a porous pipe source operated with an internal pressure of 3 psi did not exceed a radius of 4 in. during infiltration into a 4-ft. deep soil chamber. To test the agreement between experiment and model, the development of the saturated region determined in the laboratory was used as a boundary condition for computations.

The one-dimensional model gave a reasonable prediction of the advance of the wetting front horizontally when the experimentally determined growth of the saturated zone around the source was used as a boundary condition. The horizontal advance was related to time by the form $r = at^n$, where n was found to be about 0.47. Vertical advance at large times was not of this form.

The one-dimensional equation does not appear to be valid for predicting advance either vertically up or vertically down from the source. A two-dimensional solution for the entire flow region is necessary.

Although the maximum lateral extent of the wetting front occurred a few cm. below the source, the difference between the maximum lateral advance and the advance along a horizontal axis through the source was only 2 to 3 cm. Therefore, for design purposes, an accurate prediction of the advance along the horizontal axis would probably be sufficient to determine the spacing for subsurface irrigation laterals.

The effects of a plant root system and the redistribution of moisture in the soil after irrigation were not included in this study. However, observations in the laboratory indicated that redistribution in the horizontal direction was not appreciable. Therefore, if depth of subsurface irrigation laterals is determined by considerations other than the movement of the wetting front during infiltration, it may be possible to design proper lateral spacing using a one-dimensional solution of the flow equation.

VIII. RECOMMENDATIONS FOR FUTURE WORK

The results of this study should be carefully scrutinized and work undertaken to prove or disprove what has been reported here. Additional work is needed on the use of numerical procedures for calculating the moisture content distribution and advance of the wetting front around a subsurface source. Specific recommendations for future research are:

1. The two-dimensional equation describing flow from a subsurface source should be solved numerically by an efficient procedure. The more general form expressed in terms of head rather than moisture content should be used, since it theoretically applies to the saturated as well as the unsaturated region. The alternating direction explicit procedure should be investigated further and the finite element method investigated for application to this problem.

2. The applicability of the equation $r = at^n$ for describing the advance of the wetting front in the vertical direction should be tested for other soils, since the results of this study were contrary to previously published results.

3. The use of numerical procedures to predict movement from a subsurface source should be investigated for a variety of soil conditions, including layered soils and soils with nonuniform initial moisture content.

4. Field comparisons should be carried out to determine whether a solution of the diffusion equation using moisture transmission coefficients measured or estimated for field conditions can be useful for designing spacing and depth of field laterals.

APPENDIX

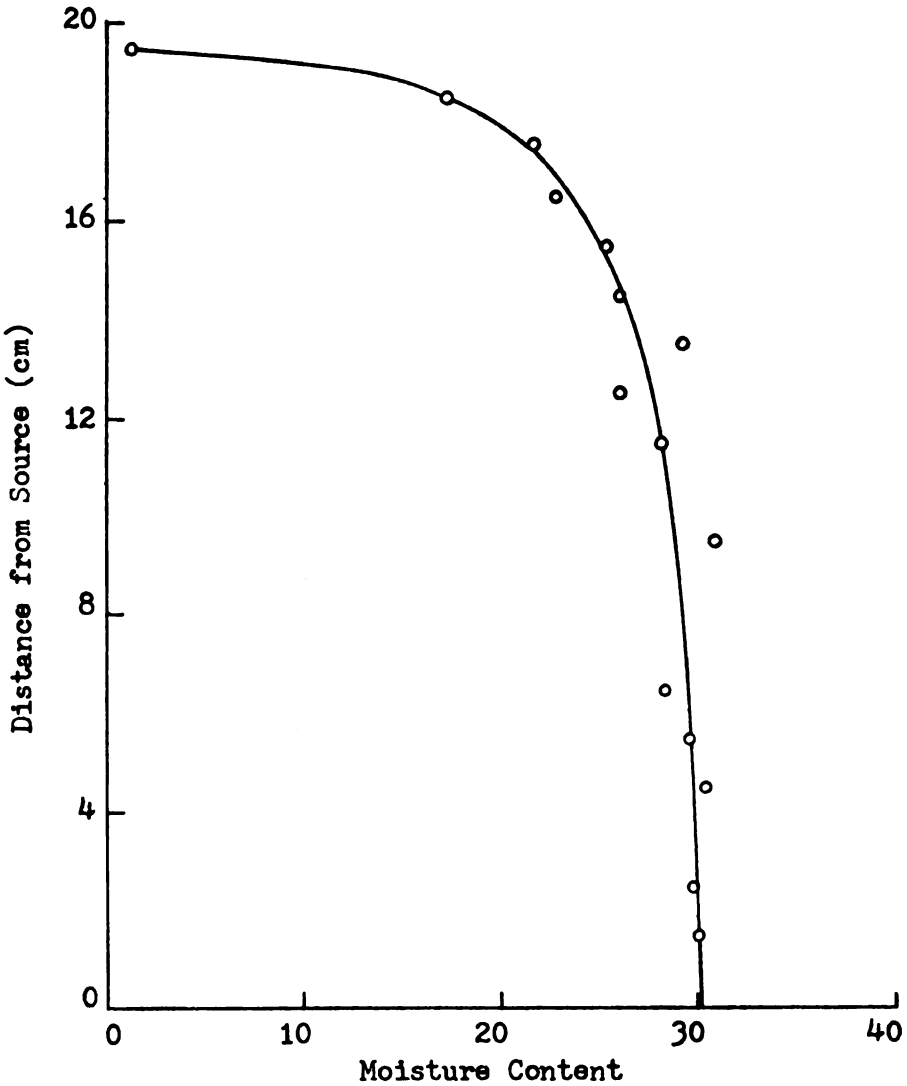

Figure 26. Distance vs. Moisture Content Relation Determined by Sectioning a Horizontal Column for Diffusivity Determination, Constant Time Method

Table 1. Data for Diffusivity by Constant Time Method

θ	x	x_2	$-\Delta x = x - x_2$	$\Delta\theta$	$-\left(\frac{dx}{d\theta}\right)_{\theta_x}$
2	19.46	19.02	.44	.15	2.93
4	19.41	18.88	.53	.15	3.53
6	19.3	18.75	.55	.15	3.67
8	19.25	18.67	.58	.15	3.87
10	19.20	18.60	.60	.15	4.0
12	19.1	18.2	.90	.15	6.0
14	18.96	17.52	1.44	.15	9.6
16	18.75	16.67	2.08	.15	13.87
18	18.42	15.8	2.62	.15	17.47
20	18.0	14.15	3.85	.15	25.67
22	17.33	10.8	6.53	.15	43.53
24	16.3	6.95	9.35	.15	62.3
26	14.8	0.9	13.9	.15	92.7
28	12.3	1.3	11.0	.05	220.0
30	3.4	24.0	21.6	.02	1080.0

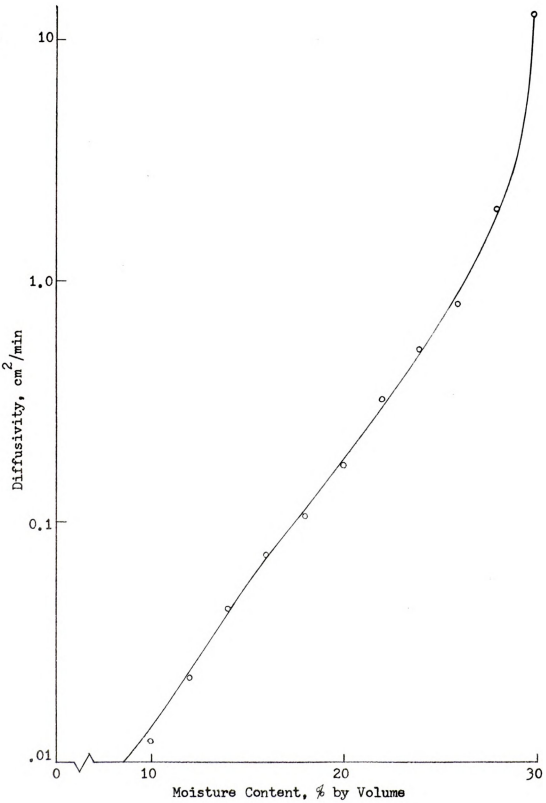

Figure 27. Diffusivity by Constant Time Method

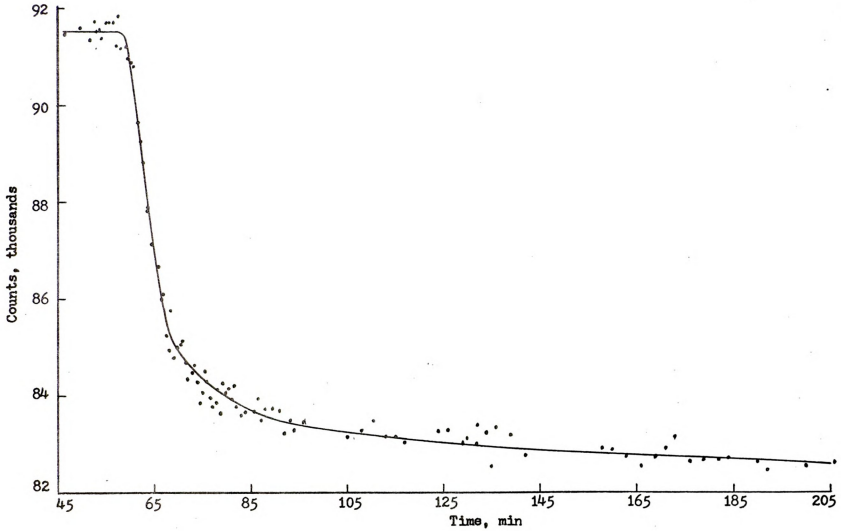

Figure 28. Gamma Ray Counts at a Fixed Position vs. Time for Diffusivity Determination

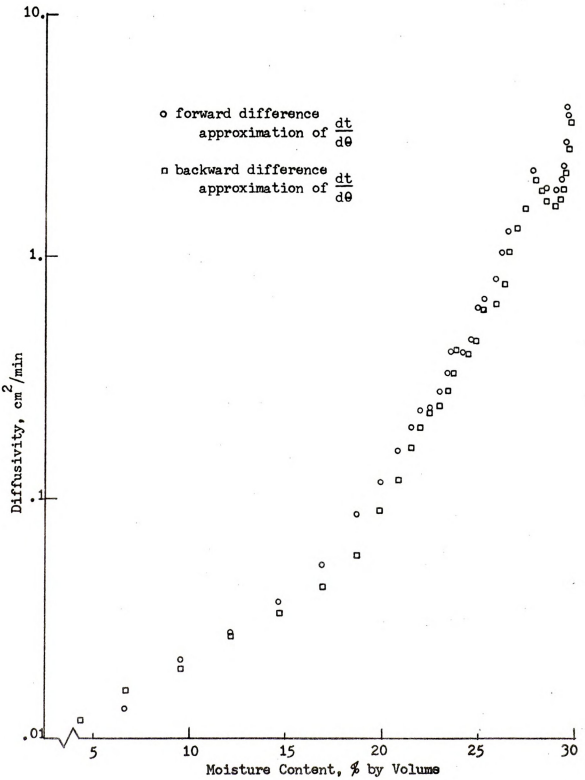

Figure 29. Diffusivity by Fixed Position Method

Table 2. Moisture Content--Capillary Pressure Head Data for Experimental Soil

Drying		Wetting	
Head (cm)	% by Volume	Head (cm)	% by Volume
0	29.9	700	17.3
24	29.7	600	17.5
41	29.4	481	17.8
55	29.2	317	18.4
70	28.6	207	19.9
86	27.6	172	20.4
100	27.0	131	21.6
115	26.2	101	22.7
130	25.6	72	24.1
146	24.8	45	25.9
161	24.1	26	27.2
190	23.3	12	29.6
220	22.4	0	30.8
270	21.5		
320	20.6		
400	19.7		
500	18.7		
600	18.0		
700	17.3		

REFERENCES

REFERENCES

Allada, S. R. and D. Quon, 1966. A stable explicit numerical solution of the conduction equation for multi-dimensional nonhomogeneous media. Chem. Engr. Prog. Symp. Series No. 64, 62: 151-156.

Brandt, A., E. Bresler, N. Diner, E. Ben-Asher, J. Heller and D. Goldberg, 1971. Infiltration from a trickle source: I. Mathematical models. Soil Sci. Soc. Am. Proc. 35: 675-682.

Braud, H. J., 1970. Surface irrigation in the southeast. Paper E-1, Proc. Natl. Irr. Symp., Univ. of Nebr., Lincoln.

Braud, H. J., T. P. Hernandez and R. T Brown, 1969. Subirrigation for greenhouse tomato production. ASAE Paper 69-228.

Bruce, R. R. and A. Klute, 1956. The measurement of soil moisture diffusivity. Soil Sci. Soc. Proc. 20: 458-462.

Brutsaert, W. F., 1971. A functional iteration technique for solving the Richards equation applied to two-dimensional infiltration problems. Water Resour. Res. 7(6): 1583-1596.

Bryan, B. and G. Baker, 1964. Small diameter plastic pipe for use in subirrigation. Ark. Farm Res. Nov.-Dec., p. 7.

Busch, C. D. and W. R. Kneebone, 1966. Subsurface irrigation with perforated plastic pipe. Trans. ASAE 9(1): 100-101.

Cisler, J., 1972. On the tensor concept of unsaturated anisotropic hydraulic conductivity. Water Resour. Res. 8(2): 525-528.

Corey, J. C., S. F. Peterson and M. F. Wakart, 1971. Measurement of attenuation of ^{137}Cs and ^{241}Am gamma rays for soil density and water content determinations. Soil Sci. Soc. Am. Proc. 35: 215-219.

Davis, S. and S. D. Nelson, 1970. Subsurface irrigation today and tomorrow in California. Paper H-1, Proc. Natl. Irr. Symp., Univ. of Nebr., Lincoln.

Douglas, J. and B. F. Jones, 1963. On predictor-corrector methods for nonlinear parabolic differential equations. Journ. SIAM 11: 195-204.

Edwards, D. M., J. D. Eastin, R. A. Olson and R. German, 1970. Subsurface irrigation today and tomorrow in the midwest. Paper G-1, Proc. Natl. Irr. Symp., Univ. of Nebr., Lincoln.

Edwards, D. M. and R. Goel, 1971. Soil moisture extraction patterns by growing plants using a subsurface irrigation system. ASAE Paper No. 71-233.

Fitzsimmons, D. W., 1972. Unsteady radial flow in partially saturated soils. Trans. ASAE 15(5): 912-918.

Freeze, R. A., 1969. The mechanism of natural ground water recharge and discharge: I. One-dimensional, vertical, unsteady, unsaturated flow above a recharging or discharging ground water flow system. Water Resour. Res. 5(1): 153-171.

Gardner, W. H., 1965. Water content. Chapter 7 in C. A. Black, Ed., Methods of Soil Analysis Part I. Am. Soc. Agron., Inc., Madison.

Gardner, W. H., G. S. Campbell and C. Calissendorff, 1972. Systematic and random errors in dual gamma energy soil bulk density and water content measurements. Soil Sci. Soc. Am. Proc. 36: 393-398.

Gilley, J. R. and E. R. Allred, 1972. Infiltration and root extraction from subsurface irrigation laterals. ASAE Paper No. 72-743.

Hanks, R. J. and S. A. Bowers, 1962. Numerical solution of the moisture flow equation for infiltration into layered soils. Soil Sci. Am. Proc. 26: 530-534.

Hanson, E. G. and B. C. Williams, 1968. Influence of subsurface irrigation on cotton yields and water use. ASAE Paper No. 68-760.

Hanson, E. G., B. C. Williams, D. D. Fangmeier and O. C. Wilke, 1970. Influence of subsurface irrigation on crop yields and water use. Paper D-1, Proc. Natl. Irr. Symp., Univ. of Nebr., Lincoln.

Hiler, E. A. and T. A. Howell, 1972. Crop response to trickle and subsurface irrigation. ASAE Paper No. 72-744.

Hoskyn, J. P. and B. B. Bryan, 1969. Subsurface irrigation research in Arkansas. Water Resour. Res. Ctr. Pub. No. 3, Univ. of Ark., Fayetteville.

Kilic, N. K., 1973. The analysis and simulation of water transfer through the soil route domain. Unpublished PhD Thesis, Dept. of Ag. Engr., Mich. State Univ., East Lansing.

Kirkham, D. and W. L. Powers, 1972. Advanced Soil Physics. John Wiley and Sons, Inc., New York. 534 p.

Klute, A., 1972. The determination of the hydraulic conductivity and diffusivity of unsaturated soils. Soil Sci. 113(4): 264-276.

Klute, A., 1965. Water capacity. Chapter 18 in C. A. Black, Ed., Methods of Soil Analysis Part I. Am. Soc. Agron., Inc., Madison.

Kriz, G. J., 1969. Temperature effects on gamma ray attenuation equipment. Trans. ASAE 12(6): 870-872, 875.

Lapp, R. E. and H. L. Andrews, 1954. Nuclear Radiation Physics. Prentice-Hall, Inc., New York. 531 p.

Lo, K. M., 1968. Orifice design and space determination for subsurface irrigation. Unpublished MS Thesis, Dept. of Ag. Engr., Univ. of Mass., Amherst.

Ozisik, M. N., 1968. Boundary Value Problems of Heat Conduction. International Textbook Co., Scranton. 505 p.

Parlange, J-Y., 1971. Theory of water movement in soils: 2. One-dimensional infiltration. Soil Sci. 111: 170-174.

Parlange, J-Y., 1972. Theory of water movement in soils: 5. Unsteady infiltration from spherical cavities. Soil Sci. 113(3): 156-161.

Patterson, T. C., 1972. Management of irrigation systems for optimizing water use efficiency. ASAE Paper No. 72-745.

Phene, C. J., G. J. Hoffman and S. L. Rawlins, 1971. Measuring soil matric potential in situ by sensing heat dissipation within a porous body: I. Theory and sensor construction. Soil Sci. Soc. Am. Proc. 35: 27-33.

Philip, J. R., 1969a. Theory of infiltration. Pp. 215-296 in Ven Te Chow, Ed., Advances in Hydroscience, Vol. 5. Academic Press, New York.

Philip, J. R., 1969b. Absorption and infiltration in two- and three-dimensional systems. Pp. 503-525 in P. E. Rijtema and H. Wassink, Ed., UNESCO Symposium on Water in the Unsaturated Zone. International Association of Scientific Hydrology, Paris. 525 p.

Qazi, A. R., 1970. Determination of capillary conductivity of unsaturated porous media for moisture characteristics. Unpublished PhD Thesis, Dept. of Ag. Engr., Mich. State Univ., East Lansing.

Raats, P. A. C., 1970. Steady infiltration from line sources and furrows. Soil Sci. Soc. Am. Proc. 34: 709-714.

Raats, P. A. C., 1972. Steady infiltration from sources of arbitrary depth. Soil Sci. Soc. Am. Proc. 36: 399-401.

Reginato, R. J. and K. Stout, 1970. Temperature stabilization of gamma ray transmission equipment. Soil Sci. Soc. Am. Proc. 34: 152-153.

Remson, I., G. M. Hornberger and F. J. Molz, 1971. Numerical Methods in Subsurface Hydrology. John Wiley and Sons, Inc., New York, 389 p.

Rubin, J., 1968. Theoretical analysis of two-dimensional transient flow of water in unsaturated and partially saturated soils. Soil Sci. Soc. Am. Proc. 32: 607-615.

Selim, H. M., D. Kirkham and M. Amemiya, 1970. A comparison of two methods for determining soil water diffusivity. Soil Sci. Soc. Am. Proc. 34: 14-18.

Sewell, John I., W. H. Allen and R. S. Pile, 1971. Visible and near infrared remote-sensing of soil moisture levels. Trans. ASAE 14(6): 1163-1166.

Smith, G. D., 1966. The utilization of a low pressure, underground water source as a method of subsurface irrigation. Unpublished MS Thesis, Univ. of Guelph, Guelph, Ontario, Canada.

Stroosnijder, L. and J. G. deSwart, 1973. Errors in soil bulk density and water content measurements with gamma ray attenuation. Soil Sci. Soc. Am. Proc. 37: 485-486.

Trambley, C. A., undated. Growing crops with Micro-Por. Micro-Por Products, a Borg-Warner Co., Chicago. 13 p.

Vachaud, G., undated. Contribution to the study of flow problems in unsaturated porous media. Unpublished PhD Thesis, Dept. of Physical Sciences, Univ. of Grenoble. (Translated by Philip Corey and A. T. Corey, Colo. State Univ., Fort Collins.)

Vaziri, C. M., 1972. Subsurface irrigation in Hawaiian sugarcane. ASAE Paper No. 72-740.

Whisler, F. D., A. Klute and D. B. Peters, 1968. Soil water diffusivity from horizontal infiltration. Soil Sci. Soc. Am. Proc. 32: 6-11.

Whitney, L. F., 1970. Review of subsurface irrigation in the northeast. Paper F-1, Proc. Natl. Irr. Symp., Univ. of Nebr., Lincoln.

Whitney, L. F., K. Muta and E. S. Pira, 1969. The effect of soil profiles on the movement of water by subsurface irrigation. Trans. ASAE 12(1): 98-99.

Whitney, L. F., E. S. Pira, C. M. Vaziri and L. F. Michelson, 1966. Water distribution from pressurized subsurface irrigation systems. Trans. ASAE 9(6): 837-838.

Wilke, O. C., 1970. Hydraulic roughness and performance of Micro-Por^{tm} pipe. ASAE Paper No. 70-724.

Zetzsche, J. B., 1964. Evaluation of subirrigation with plastic pipe. ASAE Paper No. 64-731.

Zetzsche, J. B. and J. S. Newman, 1968. The design of subirrigation laterals with uniformly spaced orifices. ASAE Paper No. 68-759.